FIRST

PROGRESS REPORT

(Project SR-109)

on

THE LOW TEMPERATURE PROPERTIES OF RELATIVELY HIGH PURITY IRON-CARBON ALLOYS

by

R. L. Smith, R. V. Fostini and R. M. Brick

UNIVERSITY OF PENNSYLVANIA

Under Bureau of Ships Contract NObs-50062

(Index No. NS-011-078)

Transmitted through

NATIONAL RESEARCH COUNCIL'S

COMMITTEE ON SHIP STEEL

Advisory to

SHIP STRUCTURE COMMITTEE

under

Bureau of Ships, Navy Department

Contract NObs-50148

(Index No. NS-731-036)

Division of Engineering and Industrial Research

National Academy of Sciences - National Research Council

Washington, D. C.

AUGUST 29, 1952

SERIAL NO. SSC-52

NATIONAL RESEARCH COUNCIL

2101 CONSTITUTION AVENUE, WASHINGTON 25, D. C.

COMMITTEE ON SHIP STEEL

OF THE

DIVISION OF ENGINEERING AND INDUSTRIAL RESEARCH

August 29, 1952

Dear Sir:

Attached is Report Serial No. SSC-52 entitled "The Low Temperature Properties of Relatively High Purity Iron-Carbon Alloys" by Smith, Fostini and Brick. This report has been submitted by the contractor as a First Progress Report on Contract NObs-50062, Index No. NS-011-078, between the Bureau of Ships, Department of the Navy and the University of Pennsylvania, covering the preliminary phase of the investigation.

The report has been reviewed and acceptance recommended by representatives of the Committee on Ship Steel, Division of Engineering and Industrial Research, NRC, in accordance with the terms of the contract between the Bureau of Ships, Department of the Navy and the National Academy of Sciences (Contract NObs-50148, Index No. NS-731-036).

Very truly yours,

P. E. Kyle

P. E. Kyle, Chairman
Committee on Ship Steel

FIRST PROGRESS REPORT

on

THE LOW TEMPERATURE PROPERTIES OF RELATIVELY HIGH PURITY IRON-CARBON ALLOYS

to

SHIP STRUCTURE COMMITTEE
via
Bureau of Ships
Department of the Navy
Contract NObs-50062
Index No. NS-011-078
Project SR-109

by

R. L. Smith, R. V. Fostini and R. M. Brick

UNIVERSITY OF PENNSYLVANIA

TABLE OF CONTENTS

ABSTRACT

The onset of brittleness in ship steel plate at a temperature which is determined by metallurgical and mechanical factors, continues to be a technical problem of considerable importance. Previous investigations of the metallurgical and mechanical factors have generally been on material equivalent to that used in actual practise; i.e. material containing a large number of compositional and stress variables. The present investigation, attempting to eliminate most of these variables, involved uniaxial tensile testing of eight relatively high purity alloys of iron containing from 0.020% to 0.49% carbon, stressed at temperatures from 28°C to those of liquid air or about -185°C. The structural conditions such as ferrite grain size and pearlite spacing were fixed and the strain rate was generally constant. The form of testing gave true stress-natural strain data. This made possible numerical evaluation of many parameters such as yield points, flow stresses, fracture stresses, ductilities in terms both of uniform and localized deformation and strain hardening factors. All of these were determined as affected by carbon content, and by temperature.

INTRODUCTION

A wealth of notched bar test data on commercial steels have been accumulated in the last ten years in the course of investigations on the general problem of low temperature brittle failures of pearlitic steel. These data have led to certain useful conclusions, e.g. that aluminum-killed steels are superior (i.e. have lower transition temperatures), that normalizing usually has a comparable beneficial effect, that fine grain size is desirable, that more than 10 ft. lbs. energy absorbed in V-notch Charpy tests at the service temperature minimizes or eliminates brittle failures, that nickel improves low temperature ductility, etc.

Useful though these conclusions are, the energy absorbed in notched bar tests is not a numerical value susceptible of analysis nor is it useful in design. Since practically all of these data have been obtained on commercial steels, too many variables are present to isolate the cause of the beneficial or detrimental effects that are observed. For example, is the beneficial effect of aluminum deoxidation attributable to a solid solution effect of excess aluminum, to the reduction or near absence of FeO, to fixing nitrogen as aluminum nitride, to a grain refining effect of

residual Al_2O_3 or to an effect of dissolved aluminum on the structure of Fe_3C in pearlite?

The investigation reported here is a part of a general program designed to answer such questions. The low temperature properties measured are uniaxial tensile properties employing customary natural stress-strain curves obtained with somewhat novel equipment. The alloys tested were made in 6 to 8 pound ingots which apart from the added element, represent 99.9 +% Fe.

PREPARATION OF IRON-CARBON ALLOYS

One general approach was to melt electrolytic iron in a magnesia crucible under air, oxidizing certain impurities, and removing them as much as possible by slagging with lime. Carbon was added by dropping sugar charcoal directly on the surface of the oxidized melt. The violence of this reaction could be controlled by adding the carbon slowly. The amount of carbon for a desired alloy had to be estimated by the boiling action in the crucible. The melt was cast into a dry graphite mold and the resulting ingot was sampled. If of satisfactory carbon content and cleanliness, it was freed from surface scale in preparation for vacuum melting.

The air melted alloys were remelted in a high-frequency vacuum melting furnace, Fig. 1. This included a 6" quartz tube with one end sealed, a brass head and 2" seamless pipe connected to the vacuum pumps through a liquid air trap to catch undesired products distilled from the furnace. The high vacuum portion could be isolated from the system by a valve to estimate the equilibrium pressure over a melt, or to preserve the vacuum during final cooling of the ingots. In order to flush the system before melting, or to melt in hydrogen or other controlled atmospheres, stopcocks were provided for connection to gas tanks and a purifying train.

A theormocouple gauge was permanently sealed into the high-vacuum manifold to continuously indicate the working vacuum. The indications of this gauge could be read either on a meter on the panel board or switched to a recording potentiometer to give a plot of the change of pressure with time. The absolute pressure was determined at intervals by means of the McLeod gauge, and these readings were used to maintain a corrected calibration of the thermocouple gauge.

Violent boiling was experienced when the previously air melted ingot became molten under vacuum. The

FeO:C reaction was finally controlled by conducting the actual melting of the solid ingot under nearly an atmosphere of evolved gases and then slowly evacuating.

SERIES I (See Table I)

Four alloys in this report, referred to later as Series I, were produced by melting in 2 1/2" x 10" diameter beryllia crucibles backed with beryllia powder contained by a graphite sleeve. It was found that if this type of crucible assembly was pre-fired in vacuo at about 1900°C and then degassed at 1550°C, satisfactory melts could be produced. These four alloys were held molten from 2 1/2 to 7 hours and were solidified under pressures ranging from 15 to 200 microns.

SERIES II (See Table I)

Solidification pressures of 15 to 200 microns indicate that carbon was continuing to react with oxygen, either FeO or BeO from the crucible. Analyses of the four alloys of Series I by the National Bureau of Standards showed oxygen contents in the range of 0.0004 to 0.0009% (see Table 1, p.33). Therefore two additional alloys were produced with improved procedures and equipment. The rather soft BeO crucibles supplied by Brush Beryllium Corporation

were fired at 1730°C, which produced a harder and therefore more slowly reacting refractory container. The graphite sleeve was omitted so that induction stirring would speed up the FeO:C reaction. An improved vacuum system was installed, substituting a DPI 275 oil diffusion pump for a mercury diffusion pump with a considerable increase in pumping speed. With these improvements, two other Fe:C alloys, referred to later as Series II, were produced with a solidification pressure of 1 micron or less.

SERIES III (See Table I)

Binary ferrites of iron with aluminum and with titanium have been produced in this laboratory using a different preparation technique and have shown exceptional ductility at liquid air temperatures. To check as to whether this ductility is a result of the specific alloying element, eg. Al, or of the procedure, one iron-carbon and one iron-carbon-aluminum alloy were produced by this alternate technique.

Electrolytic iron was melted under strongly oxidizing conditions. The metal, high in FeO, was cast as a slab which was first hot rolled and then cold rolled to a thickness of about 0.010". This

thin stock was formed into coils which were placed on BeO shells and then heated in dried (-190°C dew point) hydrogen at 1100°C for six weeks. This lengthy period has been found requisite to ensure complete deoxidation.

The hydrogen-deoxidized stock was then remelted in the high fired BeO crucibles with a sufficient amount of high purity carbon to produce the desired carbon content of 0.020%. These alloys were not successfully produced until after several attempts in which either too much or too little carbon was employed. After attaining the desired carbon and complete degassing, 0.02% aluminum was added to one alloy by dropping from the cool upper portion of the melting chamber. These alloys are later referred to as Series III alloys.

The alloys were prepared for testing as follows:

(1) The 2 1/2" diameter ingots were hot forged to one inch rounds, hot rolled at 1100°C to 5/8" square bars, cooled and surface cleaned.

(2) The bars were vacuum annealed at 1000°C for at least 100 hours to eliminate gas absorbed during hot working.

(3) The annealed stock was then cold rolled 60% to 7/16" rounds and heat treated to an equi-

axed No. 4 to 5 ASTM grain size with a medium fine pearlite spacing if the carbon content exceeded 0.03%. A strong Widmanstatten structure resulted from simple normalizing treatments. A normal structure, as shown in Figure 2, was obtained by furnace cooling in helium from austenite temperatures into the two phase $\alpha + \gamma$ region, followed by air cooling. Series III alloys (with carbon content of 0.020%) were heated in helium to the 4 to 5 grain size, attained in 50 minutes at 630°C for alloy 72V and 50 minutes at 710°C for alloy 63V. The specimens were then air cooled.

(4) The heat treated bars were then machined to four inch long tensile specimens having a one inch gauge length and a 0.252" diameter with a standard central taper (0.001"). The bars were given a final hand polish with 600 emery paper.

MECHANICAL TESTING AT LOW TEMPERATURES

The mechanical testing of the tensile specimen was done in a Baldwin Southwark hydraulic testing machine of 60,000 pounds capacity, provided with special equipment for low temperature work. This equipment was built

previously for a similar research project, and is described in references 1 and 2. However, because of some recent modifications, a brief description is given here.

The low temperature testing is conducted by submerging the specimen in a suitable refrigerant which is kept at a specific constant low temperature. The cooling fluid is contained in a Dewar vessel, supported around the test bar without interfering with the movements of the specimen grips and their alignment. Such a set-up is shown schematically in Figure 3 and can also be viewed from photograph Figure 4.

The metal Dewar, or test vessel, is supported by the movable crosshead of the machine, and therefore can, prior to testing, be moved vertically along with this cross bar into any desired position. The stem of the lower specimen grip enters the test vessel through a wide opening in the bottom with the ring-shaped space between stem and bottom being closed by light flexible bellows, (Figure 3). Thus alignment of the grips during the test can take place freely without being hindered by the rather weighty test vessel. The test bar is screwed into the bottom grip

1. H. T. Green and G. A. Moore, AISI Contribution to the Metallurgy of Steel, No. 34, 1948.
2. R. P. Steijn, M. S. Thesis, University of Pennsylvania, 1950.

from above and then the upper grip screwed downward over the threaded top part of the specimens. To provide for practically ideal self-alignment during the test, case-hardened chains are used to transfer the tensile force to the specimen, that is from the loading ram to the upper specimen grip, and from the lower grip to the movable crosshead.

The cooling media used in this investigation were liquid air for -185°C and Freon No. 12 for the range -150°C to -30°C. To cool the Freon, a copper coil carrying liquid air is fitted in the test vessel, the temperature being regulated by an automatic control circuit. To check the temperature independently at any time, an extra copper-constantan thermocouple is placed in the vessel close to the gauge section of the specimen. An air bubbler stirring arrangement is used to keep the temperature as uniform as possible.

Natural stress-strain data were obtained at low temperatures using a microformer type diameter gauge immersed with the test specimens in the heat transfer fluid, see Figure 5. The diameter gauge was calibrated against accurately machined test sections of a control bar.* The micrometer knife edges of the diameter gauge

* All dimensional data are reported in terms of inches measured at room temperature.

recorded the instantaneous diameter directly with the corresponding load on an autographic recorder. A strain pacer was connected in series with the diameter gauge and the autographic recorder. The investigator traverses the gauge length of the specimen with the jaws of the diameter gauge. While the specimen is decreasing in diameter, the diameter gauge causes the strain pacer pointer to rotate clockwise. If the spacing of the jaws of the diameter gauge increases, the pacer reverses its direction of rotation. Thus it is readily possible to find the region of necking and then to remain in the position of minimum diameter.

TEST RESULTS

Tensile data for the eight alloys are tabulated in Tables II to IX, and natural stress-strain data for five of these are presented in Figures 6 to 11. These diagrams were obtained in the conventional manner where the average instantaneous principal stress is taken as $\sigma = L/A$ and $\varepsilon = \ln A_o/A$.

σ = average instantaneous stress

ε = natural strain

L = load

Ao = original area

A = instantaneous area

A strain rate of 0.042 in. per minute (7×10^{-4} sec^{-1}) was used throughout with the exception of alloy 51V for which the strain rate varied from 0.018 in. per minute to 0.09 in. per minute as is shown in Figure 9.

From the stress strain charts, the upper and lower yield points, the flow stress at any desired strain, the fracture stress, the uniform strain (strain up to point of maximum load) and the total strain can be obtained. These properties versus the temperature of testing are plotted for six of the alloys in Figures 12 to 17. The same properties plotted versus carbon content are reproduced in Figs. 18 to 21 for fixed temperatures of 23°, -50°, -95° and -145°C. The points shown are obtained from the curves drawn through the observation points of the property versus temperature plots.

DISCUSSION OF RESULTS ON ALLOYS OF SERIES I & II

Yield points, Figures 13 to 17, increase rapidly as the temperature decreases. Double yields were observed for every temperature and every carbon content tested, although the difference between upper and lower yield points became very small for the higher carbon alloys. It can be seen that in some cases, lower

yield stresses are higher than upper yield stresses. This occurs when the amount of yield point strain is great in comparison to the drop in load, thus resulting in an apparent loss of a lower yield in the stress calculation.

Figure 18 shows that at room temperature, the yield points increase nearly linearly with carbon content. At lower temperatures, Figs. 20 and 21, there is a tendency for yield points to remain constant in the 0.1% to 0.25% carbon range. Apparently heterogeneous yielding is insensitive to carbon content in this carbon range at low temperature.

Flow stress curves for a natural strain of 0.2 are shown in Figures 13 to 17. These increase on upwardly curving lines as the temperature decreases and are similar in shape to ultimate strength curves versus temperature as typified by Figure 24. This similarity is to be expected since maximum load was generally found in the vicinity of 0.2 strain. Flow stress values were obtained at various strains for several temperatures and flow stress vs. carbon content curves were constructed as is shown in Figures 18 to 21. The flow stress for various constant

strains increases linearly with increasing carbon content up to about 0.3% carbon, then the curves tend to decrease slightly in slope from 0.3% to 0.5% carbon. The slope of the flow stress curves increases as the strain increases but remains essentially unchanged as temperature decreases.

Fracture stress values are uncorrected in any manner and were calculated from the load at fracture divided by the area at fracture as determined by post-fracture measurements made with a micrometer. Figures 13 to 17 show that the fracture stress increases as the temperature decreases to about -150°C and then falls rapidly with further decrease in temperature. This drop corresponds to a change from ductile to brittle behavior and the loss of strain hardening effects on the fracture stress.

There is a minumum of fracture stress in the vicinity of 0.05%C with a subsequent increase in fracture stress up to the 0.49% carbon alloy, Figs. 18-21. Because of the scatter in results*, it is not possible to specify with certainty the shape of

* For example, two bars of the 0.020% C alloy tested at room temperature showed as good reproducibility as could be expected - breaking loads of 970 lbs. and 930 lbs. The measured fracture diameters were 0.082 and 0.085 inches respectively with a minimum error of plus or minus 0.001 at the sharply pointed fracture. The calculated fracture stresses are 184,000 and 164,000 psi. This is about the worst divergence encountered.

the fracture stress curve versus carbon content. It appears that at room temperature, fracture stress is relatively insensitive to changes in carbon content in the range 0.05% to 0.2% carbon; whereas it increases more nearly linearly throughout the carbon range at lower temperatures. The fracture stress at liquid air temperature for most of these alloys may be taken as the fracture stress essentially unaffected by work hardening, triaxiality, changing strain rate, and structural preferment resulting from prior strain. This "unworked" fracture stress varies nearly linearly with increasing carbon content, a 0.5% C increase causing a 35,000 psi increase in fracture stress.

Total strain, uniform strain, per cent elongation and per cent reduction of area (Figures 13 to 17) remain relatively constant from room temperature to about -80°, decrease slowly from -80° to about -140°C and decrease more rapidly at lower temperatures.

Total strain decreases as the carbon content increases, Figures 18 to 21. Some of the strain may be attributed to twinning for tests conducted about -145° where both twins and deformation bands were observed. At liquid air temperatures, twinning was abundant throughout the gage section of uniform strain. It is probable

that an appreciable part of the strain at this temperature can be ascribed to twinning which is quite audible during testing.

Uniform strain is defined as the strain taking place up to the onset of necking. Its value, generally around $\epsilon = 0.20$, was taken as the strain at which maximum load occurred. Uniform strain decreases slowly with decreasing temperatures and decreases slightly with increasing carbon content.

From the plots of Figures 18 to 21, stress-strain diagrams may be constructed for iron-carbon alloys of the types of Series I and Series II for carbon contents from the range of solid solubility to 0.5% carbon and for temperatures from +23°C to -145°C. Such curves would apply to alloys with comparable microstructures and could prove useful in determining the effect of alloying elements as differentiated from the effects of carbon alone.

The property charts of Figs. 18 to 21 inclusive were initially prepared after completing tests on alloys made in the so-called Series I group. It will be recalled these were solidified under a pressure of from 15 to 200 microns and although gas contents were low (Table I), two more alloys, called

Series II, were prepared with an improved vacuum apparatus that gave solidification pressures of 1 micron or less. These alloys gave property data that plot very well indeed on the curves for properties of the earlier alloys. This generally excellent confirmation is shown in Figs. 18 to 21 by different indentification of data points for alloys of the two different series.

Since the two Series II alloys, prepared under somewhat different melting conditions from Series I and at a period nearly a year later, have properties which fall on the same graphical plots as those of the earlier series, it is felt that the two groups of alloys are of the same type and that their characteristics are reproducible. If other alloys of exactly the same carbon contents and structure were prepared, there is every reason to believe the same properties, within experimental error of measurement, would be obtained.

DISCUSSION OF RESULTS ON ALLOYS OF SERIES III

Alloys prepared by the procedure of hydrogen deoxidation followed by remelting with pure (AEC) carbon, give quite different properties; Figs. 5, 6, 11 and 12. These Series III alloys have not been plotted

on the summary plots of Figs. 18 to 21 since they appear to be different materials. For example, a comparison of Figs. 11 and 13, 0.020% C and 0.023% C, series III and II respectively, reveals that the series III material showed a 50% higher yield point, a considerably higher total strain, and relatedly, a vastly higher fracture stress.

A comparison of Figs. 11 and 12, both Series III alloys with 0.020% carbon but one, alloy 63V, containing 0.02% aluminum, shows that these two series III alloys have nearly identical properties. It is concluded that, under these particular conditions of alloy preparation, aluminum has no beneficial effect. This appears to support the concept that the usual role of aluminum in steels is to remove oxygen, neutralize nitrogen and refine the grain size; i. e. that it has no significant "alloying" effect of its own in the usual concentration range.

The superior ductility of the Series III alloys of this report is apparently quite reproducible.

This laboratory has produced other ferrites, e.g. pure iron plus about 0.02% Al or 0.02% Ti, and

customarily obtains good ductility at liquid air temperatures. These alloys, substantially carbon free, have shown 50 to 60% reduction of area at -183°C, i.e. well defined necking. Without carbon, these alloys have much lower yield points than the iron-carbon alloys of this report and lower than any of those of the National Physical Laboratory. These alloys are not included in this report but are cited to emphasize that the exceptional ductility of the present Series III alloys is not a freak result but is characteristic of alloys prepared and heat treated by Series III procedures.

The problem remains to explain the considerable difference in properties of the two carbon alloys made by different procedures, having shown that each type is apparently reproducible. One possible line of reasoning is as follows:

(1) Carbon is not the significant variable; the 0.003 points difference between 0.020% (Series III, alloy 72V) and 0.023% (Series II, alloy 56V) is almost within the experimental error of precision chemical analysis.

(2) Oxygen, nitrogen and hydrogen are not the significant variables since again the total amount present of each is very small and even though hydrogen deoxidation may have been more effective, subsequent vacuum melting in BeO always resulted in some oxygen pick-up. Hydrogen is removed both by this oxygen, by the vacuum (solidification pressure of 1 micron) and in any case, would not give the observed property effects.

(3) Analyses for other elements as listed in Table I reveal no differences in composition to which the property differences may clearly be attributed.

(4) One difference between the Series III alloys and the others was exposure to BeO. Attempting to obtain the desired 0.020% C required five vacuum remelts, made in the same BeO crucible, before the desired carbon content was attained but the differences in metallic beryllium

content do not appear to be significant.

(5) The alloys of Series III were heat treated differently. All others, including the 0.023% C Series II alloy, were heated above the A_3 temperature, furnace cooled to above the A_1 and then air cooled. The two Series III alloys of only 0.020% C became too coarse grained from this heat treatment. To attain the desired ASTM grain size, they were recrystallized below the A_1 (630°C for alloy 72V; 710°C for alloy 63V) and air cooled, presumably at the same rate through the carbide precipitation range as all other alloys.

COMPARISONS WITH OTHER DATA

At the moment, no reason for the difference between Series II and Series III alloys can be given. Since the difference appears to be reproducible, work in the immediate future will be concentrated on this point.

The National Physical Laboratory of England has been carrying on work in the same field as that reported here and a recent publication* makes it possible to compare

* W. P. Rees, B. E. Hopkins and H. R. Tipler - "Tensile & Impact Properties of Iron and some Iron Alloys of High Purity" Journal Iron and Steel Institute, October 1951.

data from the two investigations. In general, the properties of their iron-low carbon alloys that were melted in 25 pound heats compare with our Series II irons. An alloy of theirs with 0.01%C had a yield point and fracture s tress that fall reasonably well on an extrapolation of our Series II data. Their lowest V-notch Charpy transition temperatures of around -15°C are between the -36°C for our series III alloys and -6°C for Series II low carbon heats. None of their alloys showed more than 5% tensile elongation at -196°C although our Series III alloys showed 29% at -183°C with about 40% reduction in area.

However, all of their small (6 lbs.) heats, frozen in the furnace and comparable in that respect to ours, were far more brittle than any alloys tested here. Brittleness, e.g. only a 15% reduction in area at room temperature, was attributed to oxygen even though only 0.0007% was reported as present by analysis. While the National Physical Laboratory 6 lb. heats compare with ours in size and freezing method, the alloys are not really comparable since the brittleness

they encountered was intergranular and therefore differs in kind from the low temperature brittleness forming the subject of this investigation.

It is desirable to compare these data on high purity iron-carbon alloys with the room temperature properties recently reported by the Naval Research Laboratory* for experimental steels containing from 0.01% to 0.60% C with approximately 1.0% Mn and 0.25% Si. Figure 23 shows that their reported yield points are consistently about 15,000 psi above those for our Series I and II alloys. They obtained greater total strains and relatedly appreciably higher fracture stresses. Our Series III alloys were lower in yield strength and more ductile than those of the Naval Research Laboratory. It is unexpected to find both lower strengths and lower ductilities for the purer alloys (Series I and II). Unfortunately, this difference cannot be ascribed solely to compositional differences, particularly manganese, since the purer alloys reported here were coarser grained, ASTM No. 4 to 5 as compared to ASTM No. 8 for alloys tested by the

* Raring, Rinebolt and Harris, Journal of Metals, May 1951, p. 395; Also ASM Preprint 33, 1950.

Naval Research Laboratory. Apart from the differences in absolute values for stresses and strains, both investigations show similar effects of carbon on room temperature properties of the pearlitic structures tested.

Finally, tensile properties of the lowest carbon content iron-carbon alloys may be compared with those of some pure binary ferrites prepared and tested on a companion program in the same laboratory. None of the Series I or II iron-carbon alloys show ductility at any temperature in the range 23° to -185°C that is as high as that for pure ferrites containing 0.02 to 0.2% aluminum or 0.02 to 0.2% titanium. The Series III alloys have almost as good ductility as the aluminum or titanium ferrites, but have nearly three times as high yield strength.

STRAIN HARDENING & TRANSITION TEMPERATURES

In discussing properties derived from the portion of the stress-strain diagram after necking begins, it should be recognized that the effects of triaxiality, varying strain rate, plastic deformation and varying degrees of structural preferment are acting on the test specimen.

It should be further emphasized that the stress-strain diagrams as usually constructed are plots of the average axial principal stress versus natural strain at the minimum diameter of the test bar.

The method used for the tests described in this report for controlling the strain rate was to maintain a constant rate of head motion of the testing machine, thus keeping the rate of longitudinal extensions constant. Since natural strain is defined as ln l/l_o or ln A_o/A, it can be seen that a constant rate of head motion results in a much greater rate of natural strain as the severity of necking increases. Both increasing the strain rate and setting up a condition of triaxiality have the same general effect as decreasing the temperature in that stress levels for particular strains are increased, total strains are decreased and uncorrected fracture stresses are increased. This is the reason for the upturn of the stress-strain curves in Figure 6, near the end of each test.

Some experiments have been performed to adjust for the change in natural strain rate during necking. When the strain rate is decreased to the same value as that employed at the point of maximum load, the

flow stress drops abruptly and remains at a lower level. Increasing the strain rate to the original constant head motion raises the flow stress to the appropriate position on the original flow curve.

Attempts have been made to correct the natural stress-strain curves for triaxiality using both the Bridgman correction and a correction developed here. This latter is based on the observation that the average stress at a section of the neck away from the minimum diameter is not on the stress-strain curve for the indicated lesser strain but has a lower value and the difference may be attributed to triaxiality. Our corrected stress-strain curves are not yet sufficiently complete to permit any conclusions to be included in this report.

Both corrected and uncorrected natural stress-strain curves have been analyzed for the so-called modulus of strain hardening and the strain hardening index n. Analyses of uncorrected curves reveal a consistent slight increase in strain hardening of the iron-carbon-alloys as temperature decreases from 23°C to -150°C. However, this may be only an apparent effect since neither the corrected

stress-strain curves nor micro hardness tests confirm any such effect.

The drop in fracture stresses of Figures 12 to 17 was previously stated to be caused by a change from ductile to brittle behavior. The temperature of this change, or the transition temperature of an Fe-C alloy, may be determined in several ways. The usual basis for stipulating transition temperatures is the energy to fracture. This was determined for the axially loaded, unnotched tensile test bars by graphical integration of the area under the uncorrected natural stress-strain curves of Figs. 6 to 11. The plots of E_f or energy to fracture vs. temperature give curves which are approximately parallel to the total strain vs. temperature curves. The E_f curves are nearly horizontal in the range +23°C to -140°C with a slight maximum within this range; then they decrease sharply to a low value at -185°C. The transition temperature was chosen as that at which E_f was half of the maximum value. Figure 23 shows a plot of transition temperature vs. per cent carbon for Series I & II alloys. A nearly horizontal line showing no effect

of carbon content (in the range 0.023% to 0.5%) on the transition temperature of un-notched specimens satisfactorily represents the data, considering the error in individual points.

Series III alloys are not plotted in Fig. 23 but their transition temperatures, defined as above, would also be in the range, -160 to -170°C, despite their greater ductility at liquid air temperatures. Separate analyses for transition temperature based on maximum fracture stress or total strain lead to the same conclusion as to the absence of a carbon effect on transition temperature of un-notched specimens. However it is noted that the energy to fracture at room temperature and the maximum energy to fracture both decrease sharply with increase in carbon content and are higher for the more ductile Series III alloys.

Notched bar tests were run on five of the eight alloys covered by this report. The 7/16" cold rolled bar stock was given a cold pass through 90° grooves in rolls to produce a square 0.430" bar. This stock

was annealed to the same micro-structure as the tensile test bars, No. 4-5 ASTM grain size, and machined into standard V-notch Charpy test bars which were broken over a range of temperatures. The test data are reproduced in Fig. 25 and transition temperatures for 15 ft. lbs. as a criterion and for 60 ft. lbs. which generally corresponded to a 50% brittle fracture, are reproduced below.

V-Notch Charpy Transition Temperatures

	Alloy 72V Series III 0.020% C	Alloy 63V Series III 0.020% C +0.020% Al.	Alloy 56V Series II 0.023% C	Alloy 49V Series I 0.05% C	Alloy 58V Series II 0.22% C
15 ft.lbs.	-47.°C	-40.°C	-6.°C	37.°C	32.°C
60 ft. lbs.	-36.	-36.	21.	65.	72.

SUMMARY & CONCLUSIONS

Eight iron-carbon alloys of relatively high purity, 99.9+% Fe with from 0.02 to 0.49% carbon, were produced using three different procedures. All procedures appeared to give alloys of substantially equivalent purity and in particular, all alloys had

very low oxygen and nitrogen contents i.e. in the range 0.000X%.

Natural stress-strain data were obtained over a range of temperatures from +23°C to -185°C on these alloys, which had microstructures with ASTM No. 4-5 ferrite grain size and pearlite, if present, of spacing equivalent to normalized steels. Five of the alloys were tested for Charpy V-notch transition temperatures. Analyses of these data lead to the following conclusions:

(1) Yield points and flow stresses increased with increase of carbon content and with decrease in temperature.

(2) Fracture stresses also increased with increase in carbon content and with decrease in temperature until, at around -150°C, loss of ductility became pronounced and with less strain hardening, the fracture stress dropped to a considerably lower value at -185°C.

(3) Ductility, as indicated by total strain to fracture, remained relatively constant from room temperature to about -80°C, decreased slowly to around -140°C and then

very rapidly dropped to approach zero at -185°C although the Series III alloys still showed appreciable ductility at this temperature. Ductility at any temperature in this range decreased with increase in carbon content.

(4) The transition temperature, based on half of the maximum energy to fracture of unnotched, axially loaded tensile specimens, was at about -160° to -170°C for all carbon contents investigated. Above this temperature, energy to fracture decreased sharply with increase in carbon content.

(5) The transition temperature of V-notched Charpy bars decreased with decrease in carbon content, reaching about -36°C for Series III alloys.

(6) Strain hardening, as indicated by the slope of the uncorrected natural stress strain curves, increased slightly as the temperature of straining decreases. However when corrections were made for triaxiality of stress during necking, there was no clearly defined effect of temperature on strain hardening.

(7) The foregoing tensile properties appeared to be reproducible in irons produced by similar procedures. A change in production method and heat

treatment (Series III alloys) considerably altered properties, giving higher ductility and also higher yield and flow stresses at all temperatures for equivalent carbon content. Aluminum, in these oxygen-free alloys, was not significant in achieving the pronounced alteration of properties.

(8) The iron-low carbon alloys of our Series III had pronouncedly higher ductilities at all temperatures and lower transition temperatures than comparable irons produced at the National Physical Laboratory in England. The reason for our markedly better low temperature properties is not now certain.

FUTURE WORK

1. The pronounced difference in low temperature properties of Series II and Series III alloys requires explanation since the subtle effect operating here would seem to be very important to the general problem

of low temperature behavior of ferritic steels. It is proposed that more Series II type low carbon content alloys be prepared and heat treated by Series III procedures - and vice versa. Furthermore the effect of varied temperatures and cooling rates of Series III alloys, still at a constant ferrite grain size, should be investigated.

2. Since it appears probable that the interstitial solutes, carbon and nitrogen, are significant in controlling low temperature properties, internal friction measurements should be made to determine the state and distribution of these elements.

Table I

Analyses of Iron-Carbon Alloys

	Alloy 72V (Series III)	Alloy 63V (Series III)	Alloy 56V (Series II)	Alloy 49V (Series I)	Alloy 51V (Series I)	Alloy 58V (Series II)	Alloy 43V (Series I)	Alloy 53 (Series I)
Pressure (Microns)	0.6	1.5	1.0	200.	30.	0.8	15.	200.
Al	---	0.020	---	--	--	---	--	---
C	0.020+	0.020+	0.023+	0.05	0.12	0.22	0.25	0.49
Mn (Spectrographic)	0.0005	0.0005	0.0005	---	---	0.0005	---	---
Mn (Wet method)	0.003	0.001	0.002	0.002	0.002	0.003	0.002	0.002
P	---	---	---	0.006	0.005	---	0.006	0.005
S	---	---	---	0.004*	0.003*	---	0.001*	0.004*
Si	0.005	0.002	0.001	0.001	0.005	0.005	0.001	0.005
Be	0.0013	0.006	0.0007	0.005	---	0.0013	---	---
Ni	0.0008	<0.0003	<0.0003	---	---	0.0008	---	---
Cr	0.0004	0.0004	0.0004	---	---	0.0004	---	---
O(NBS)*	0.0006	0.0008	0.0007	0.0004	0.0003	0.0002	0.0007	0.0008
(BMI)+	0.0010	0.0003	0.0014 (.0038)	0.0006	---	0.0005	---	---
N(NBS)*	0.0008	0.0010	0.0011	0.0016	0.0012	0.0007	0.0008	0.0009
(BMI)+	0.0003	0.0002	0.0004	0.0004	---	0.0004	---	---
H(NBS)*	nil	0.00003	0.00007	nil	0.00009	nil	0.0002	0.00012
(BMI)+	<0.00004	<0.00004	<0.00004	<0.00004	---	<0.00004	---	---

* Average of duplicate vacuum fusion analyses by National Bureau of Standards, courtesy J. G. Thompson

\+ Duplicate vacuum fusion analyses by Battelle Memorial Institute, courtesy C. E. Sims

Wet manganese analyses by Balke Research Associates.

All other analyses by W. B. Coleman Inc.; spectrographic method for metallic elements

Note: The amount of each element present, other than carbon, is near the limit of experimental error of the available analytical methods. Therefore although two to four times as much nitrogen or oxygen, for example, is reported by one laboratory as compared to another, the differences generally are not significant since the amount present is in the vicinity of .000X%

Number of Bar No.	Test Temperature °C	Upper Yield Point psi.	Lower Yield Point psi.	Fracture Stress psi.	Flow Stress at Natural Strain of 0.2 psi.	Uniform Strain	Total Strain	Ultimate Strength psi.	Elongation in One Inch %	Reduction in Area %
10	+23	31,800	26,950	183,700	47,000	.382	2.028	40,700	53	89
9	+23	30,800	27,600	164,000			2.150	40,600	52	88
5	-29	37,200	34,100	206,500		.332	2.35	44,400	56	90
13	-29	43,400	34,300	215,000	53,000	.366	2.397	44,100	56	91
2	-89	57,500	50,800	210,000	65,000	.192	2.17	53,700	60	89
8	-152	85,400	77,500	196,000	99,700	.178	1.41	82,000	-	76
1	-153	84,700	77,800	200,000	98,500	.185	1.47	81,200	41	77
7	-183	94,800	92,100	153,000	123,000	.177	.544	101,000	27	39
11	-183	92,400	93,400	149,800	121,500	.185	.492	101,000	29	42
4	-183	94,100	93,700	139,000	125,000	.181	.361	102,000	29	30.5

Table II

Strain rate for all bars
.04 in./in./min.

Tensile data for iron - 0.02% Carbon alloy
(Series III; solidified under pressure of 0.6 micron)

Number of Bar No.	Test Temperature °C	Upper Yield Point psi.	Lower Yield Point psi.	Fracture Stress psi.	Flow Stress at Natural Strain of 0.2 psi.	Uniform Strain	Total Strain	Ultimate Strength psi.	Elongation in One Inch %	Reduction in Area %
12	+23	36,800	29,000	205,000	52,000	.370	2.213	43,400	45	89.5
16	+23	36,390	28,400	195,000	52,000	.314	2.161	43,000	42	82
13	+23	36,000	28,500	197,500	49,000	.351	2.192	42,400	48	89
5	+23	35,900	28,450	198,500	51,500	.382	2.266	42,500	45.5	89.5
3	-30	43,300	35,900	204,000	56,000	.380	2.19	46,600	56	91
11	-30	39,000	35,900	196,000	57,000	.317	2.145	47,400	56	88.5
10	-90	63,600	60,200	206,000	72,000	.270	1.924	59,250		85.5
7	-90	61,500	53,900	217,000	70,500	.220	2.10	57,100	53	89.5
15	-90	62,100	55,000	187,500	65,500	.264	1.924	56,300	51	85.5
6	-150	85,500	79,500	185,000	101,000	.185	1.370	83,000	33	74.5
14	-152	84,300	82,500	181,000	103,500	.189	1.239	84,200	36	71
4	-158	85,600	82,600	183,500	105,500	.182	1.215	86,800	31	70.5
1	-183	92,000	93,000	144,500	126,000	.199	.401	102,800	23.5	35
8	-183	92,000	94,100		127,500	.200		104,000		
9	-183	93,500	93,600	145,000	126,500	.195	.412	103,300	26	33.5

Strain rate for all bars .04 in./in./min.

Table III

Tensile data for iron - 0.02% Carbon + 0.02% Aluminum alloy (Series III; solidified under pressure of 1.5 microns)

Number of Bar	Test Temperature	Upper Yield Point	Lower Yield Point	Fracture Stress	Flow Stress at Natural Strain of 0.2	Uniform Strain	Total Strain	Ultimate Strength	Elongation in One Inch	Reduction in Area
No.	°C	psi.	psi.	psi.	psi.			psi.	%	%
20	+23	19,610	19,250	120,500	50,500	.314	1.503	41,800	50	78
16	-29	29,600	27,400	132,900	57,000	.209	1.521	46,200	53	78
24	-29	28,900	27,500	125,200	57,000	.272	1.522	46,100	53	78
26	-87	47,400	46,100	146,500	68,000	.292	1.429	56,200	52	77
17	-91	52,900	47,400	139,000	69,500	.224	1.410	57,900	50	76
22	-149.5	79,700	75,700	147,200	97,500	.182	.98	80,500	37.5	62.5
18	-151	81,900	77,600	113,900	102,500	.175	.370	84,600	28	32.5
23	-183	95,700	95,500	103,000			.06		6	6
19	-183	93,800	95,200		Bar broke on shoulder					

Strain rate for all bars
.04 in./ in./min.

Table IV

Tensile data for iron - 0.023% Carbon alloy
(Series II; solidified under pressure of 1 micron)

Number of Bar No.	Test Temperature °C	Upper Yield Point psi.	Lower Yield Point psi.	Fracture Stress psi.	Flow Stress at Natural Strain of 0.2 psi.	Uniform Strain	Total Strain	Ultimate Strength psi.	Elongation in One Inch %	Reduction in Area %
4	+23	21,200	20,600	115,200	53,500	.330	1.378	44,700	42	75
10	+23	20,500	none	115,800	54,500	.274	1.348	45,200	41	75
1	-49	35,900			60,100					
=	-47		33,600							
=	-49			126,000		.339	1.376	49,800	52	74
14	-49	36,600	35,600	125,100	62,500	.322	1.313	51,600	52	73
2	-89	53,700	51,500	127,000	72,500	.239	1.23	59,300		71
5	-97	54,600			74,000					
=	-92		53,200	109,800		.208	.911	60,600	47	60
8	-96	55,800	55,200		73,500					
=	-93			134,900		.256	1.240	60,200	48	71
6	-150	83,600	79,200	133,900	101,000	.196	.765	82,500	25	54
9	-152	85,100	79,000	126,400	103,000	.185	.551	83,700	22	43
13	-147	85,200	80,700	148,100		.187	.895	83,700		58
11	-183	97,400	99,600	102,300			.049	96,300	6	5
7	-183	97,100	98,600	103,700			.054	97,200	9	5

Strain rate for all bars
.04 in./in./min.

Table V

Tensile data for iron - 0.05% carbon alloy
(Series I; solidified under pressure of 200 microns)

Number of Bar	Test Temperature	Rate of Strain	Upper Yield Point	Lower Yield Point	Fracture Stress	Flow Stress at Natural Strain of 0.2	Uniform Strain	Total Strain	Ultimate Strength	Elongation in One Inch	Reduction in Area
No.	°C	in./min.	psi.	psi.	psi.	psi.			psi.	%	%
35	+ 23	0.025	28,000	26,100		61,300	0.350	0.967	51,000	38	63
24	+ 23	0.025	28,800	26,600	114,800	61,000	0.329	1.083	51,000	39	66
45	+ 23	0.05	30,100	27,100	104,200	63,000	0.332	0.925	52,000	39	63
19	+ 23	0.018	27,400	25,400	107,300	61,500	0.336	1.012	51,000	38	64
23	- 55	0.05	43,600	40,100		73,000	0.291		59,000	42	66
=	- 51				129,800			1.077			
44	- 55	0.05	45,100	41,900		73,700	0.281		61,000	45	60
=	- 50				130,300			1.044			
36	- 93	0.05-0.025	61,100	57,400	134,000	83,300	0.207	1.008	70,000	42	63
41	- 98	0.05-0.025	61,300	56,600		84,600	0.275		69,000	42	61
=	- 98				134,000			0.940			
20	- 95	0.04	58,500								
=	- 90			55,000	135,200	80,200	0.220	0.993	65,500		63
49	-147	0.05-0.025	90,100	86,600	139,200	107,300	0.228	0.657	89,000	38	54
32	-148	0.05-0.025	89,700	87,000		109,000	0.211		89,000	39	50
=	-147				140,400			0.702			
28	-147	0.04	87,900	82,600	143,200	105,000	0.212	0.767	86,500	32	53
31	-188	0.05	105,300	106,000	111,000		0	0.070	104,000	3	5
27	-188	0.05	105,800	106,800	116,200		0	0.094	109,000	6	8

Table VI

Tensile data for iron - 0.12% carbon alloy (Series I; solidified under pressure of 30 microns)

Number of Bar No.	Test Temperature °C	Upper Yield Point psi.	Lower Yield Point psi.	Fracture Stress psi.	Flow Stress at Natural Strain of 0.2	Uniform Strain	Total Strain	Ultimate Strength psi.	Elongation in One Inch %	Reduction in Area %
28	+23	29,700	29,400	118,600	74,000	.276	.79	61,000	36	55
22	+23	28,350		107,200	71,000	.211	.733	58,200	37.5	54
23	-29	34,800	34,900	122,300	81,500	.221	.736	66,900	37.5	52.5
29	-29	35,800	35,800	132,500	83,000	.206	.79	68,700	41	55.5
31	-89	56,600	57,700	132,800	98,000	.224	.636	80,500		47.5
24	-89	58,100	57,000	125,500	96,000	.214	.598	78,400	--	46
27	-150	90,700	88,800	136,000	121,500	.1865	.337	101,800	41	29
26	-152	97,800	93,100	142,000	126,000	.160	.396	103,800		33
25	-183	120,500		121,500			.008		0	1
32	-183	120,500		120,000			.024		2	2.5

Strain rate for all bars
.04 in./in./min.

Table VII

Tensile data for iron - 0.22% Carbon alloy
(Series II; solidified under pressure of 0.8 micron)

Number of Bar No.	Test Temperature °C	Upper Yield Point psi.	Lower Yield Point psi.	Fracture Stress psi.	Flow Stress at Natural Strain of 0.2 psi.	Uniform Strain	Total Strain	Ultimate Strength psi.	Elongation in One Inch %	Reduction in Area %
19	+23	31,950	31,400	119,300	76,200	.239	.782	62,400	36	59.2
7	+23	32,000	31,900	114,700	78,000	.221	.761	63,500	34	53.3
26	-29	39,300	37,400	124,700	86,000	.252	.742	70,500	32	52.5
14	-29	38,700	37,400	127,200	85,000	.258	.790	69,800	37	54.7
23	-52	45,400	43,600							
=	-54			124,200			.715		38	51
15	-57	46,100	44,600		89,000	.210		73,100		
=	-56			128,500			.706		43	51.5
18	-90	57,700	55,700	132,000	97,500					
=	-88					.207	.686	79,500	30	49.6
6	-92	57,500								
=	-94		57,500	134,500	100,000	.195	.678	82,700		49.2
11	-149	90,700	89,300		125,000					
=	-148			150,700		.220	.524	102,500	22	40.8
27	-149	87,800		149,500	123,200	.160	.557	101,400	25	42.7
10	-185	120,200		121,000			.019	119,200	2	2
22	-185	120,800		116,600*			.019	120,000	2	2

Strain rate for all bars
.04 in./in./min.

Table VIII

Tensile data for iron - 0.25% carbon alloy.
(Series I; solidified under pressure of 15 microns)

Number of Bar	Test Temperature	Rate of Strain	Upper Yield Point	Lower Yield Point	Fracture Stress	Flow Stress at Natural Strain of 0.2	Uniform Strain	Total Strain	Ultimate Strength	Elongation in One Inch	Reduction in Area
No.	°C	in./min.	psi.	psi.	psi.	psi.			psi.	%	%
7	+23	.04	40,800	41,100	120,600	98,500	.213	.443	81,300	27	36
23	+23	.04	42,600	none	130,200	105,000	.217	.504	84,800	27	40
15	-46	.04	55,600	none		118,000			97,000		
=	-48	.04			141,800		.201	.463		25	38
3	-48	.04	51,500	51,400		116,700					
=	-49	.04			135,000		.208	.417	95,000	27	33
27	-94	.04	67,000	67,500		122,500					
=	-95	.04			143,500		.223	.457	101,100	28	37
12	-95	.04	71,300	71,800	144,200	127,000	.180	.379	104,100	27	30
24	-151	.04	106,600	Broke on shoulder							
4	-150	.04	106,000	107,000	160,000	156,000	.138	.229	128,000	9	20
16	-185	.04			138,700		.008	.008	137,700	0	0
11	-185	.04	133,000		135,200		.016	.016	133,000	0	0

Table IX

Tensile data for iron - 0.49% carbon alloy.
(Series I; solidified under pressure of 200 microns)

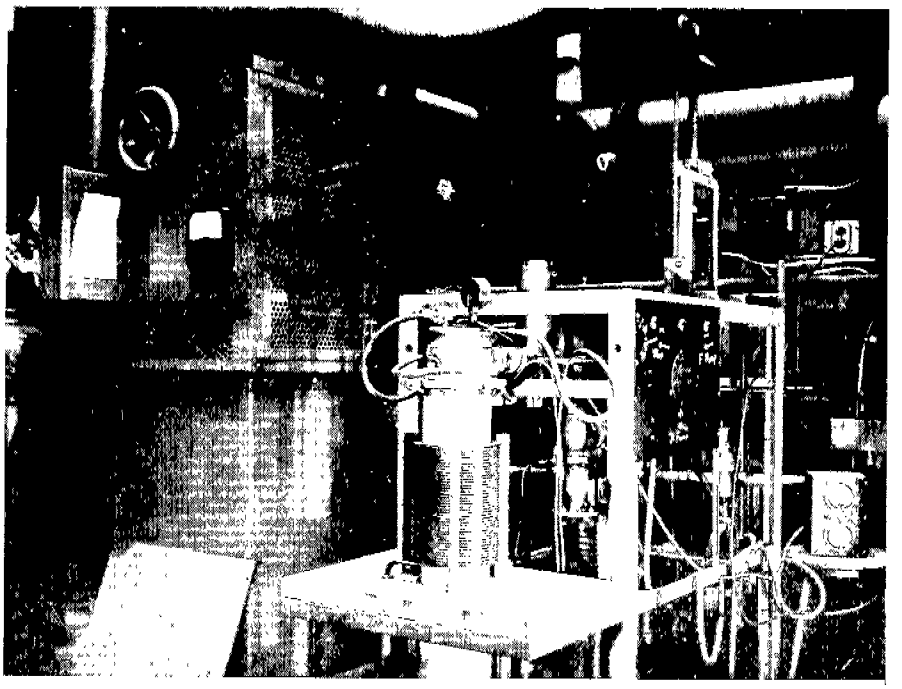

FIGURE 1: High Frequency Induction Vacuum Furnace

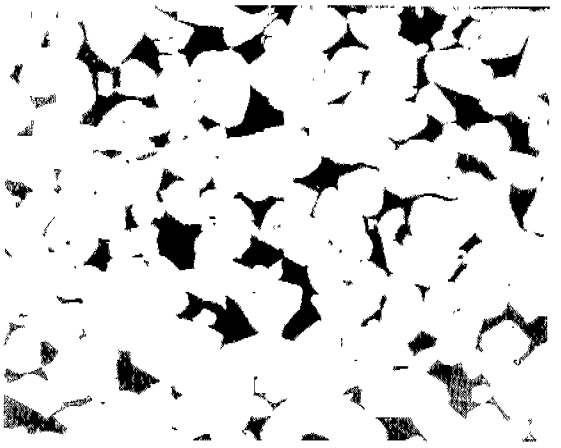

FIGURE 2: Structure of 0.12% carbon-iron alloy (51v) held 15 minutes at 900°C and furnace cooled to 780°C, held ten minutes, then air cooled; x100 Nital etch.

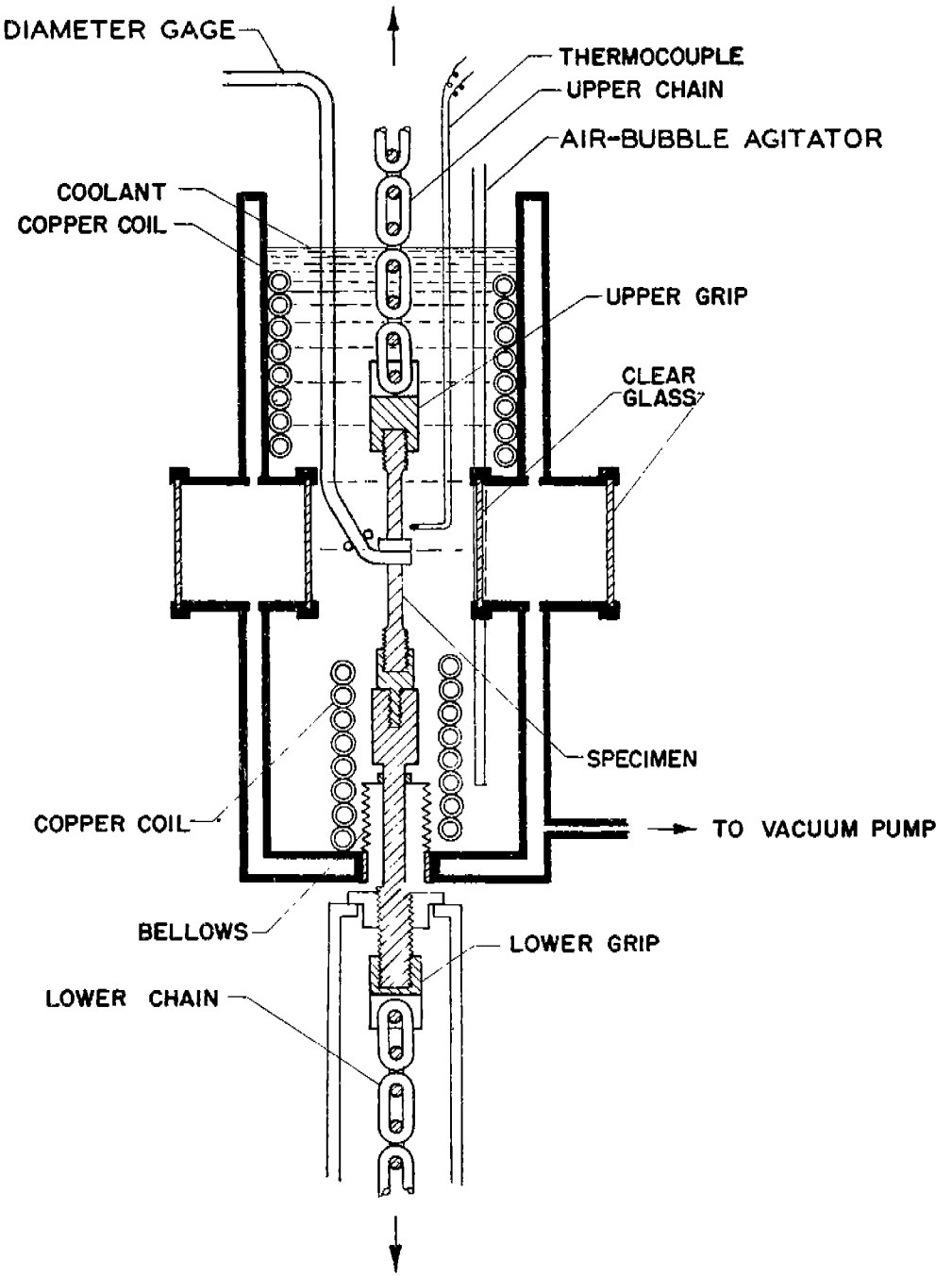

FIG. 3 SCHEMATIC DIAGRAM OF TENSILE TEST APPARATUS

J.W.

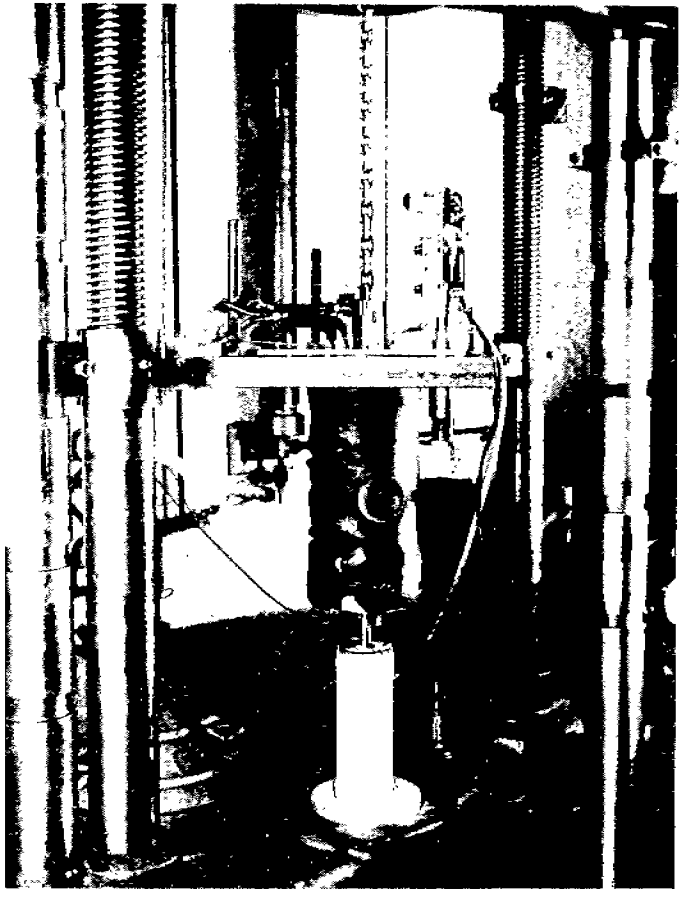

FIGURE 4: Low Temperature Tensile Test Apparatus

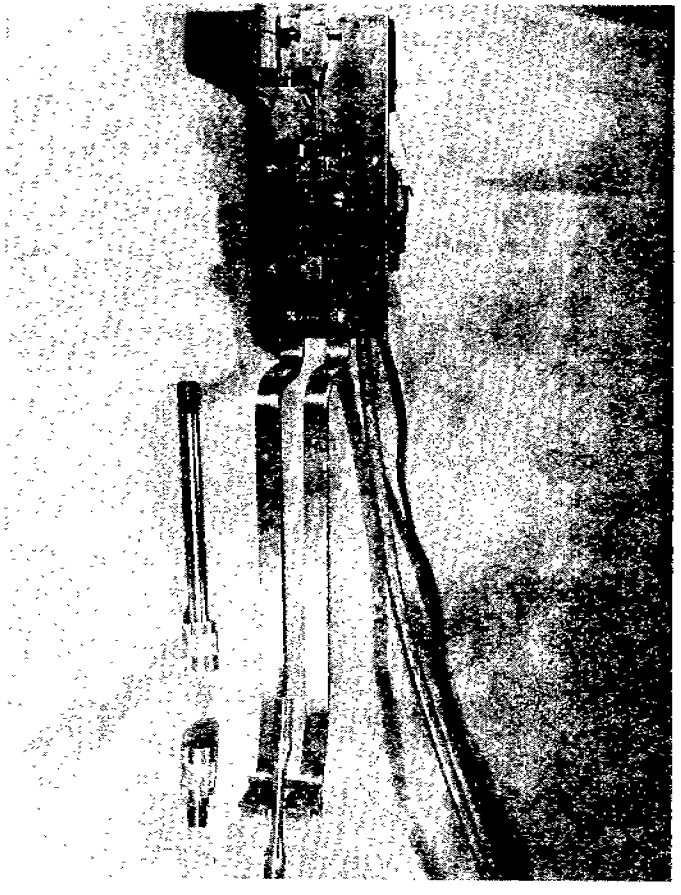

FIGURE 5: Diameter Gauge Used in Tensile Testing

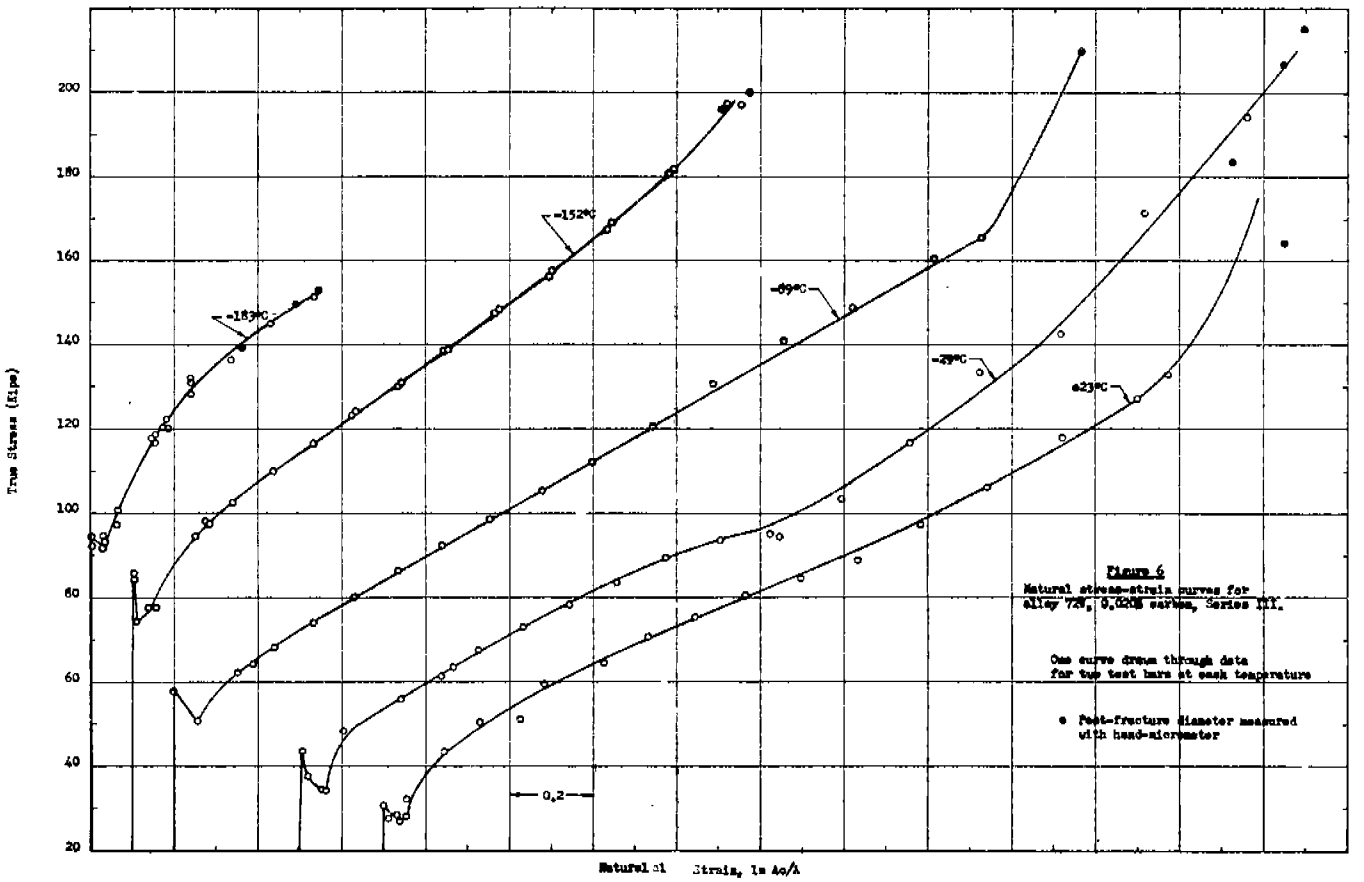

Figure 6
Natural stress-strain curves for alloy 72W, 0.02% carbon, Series III.

One curve drawn through data for two test bars at each temperature

• Post-fracture diameter measured with hand-micrometer

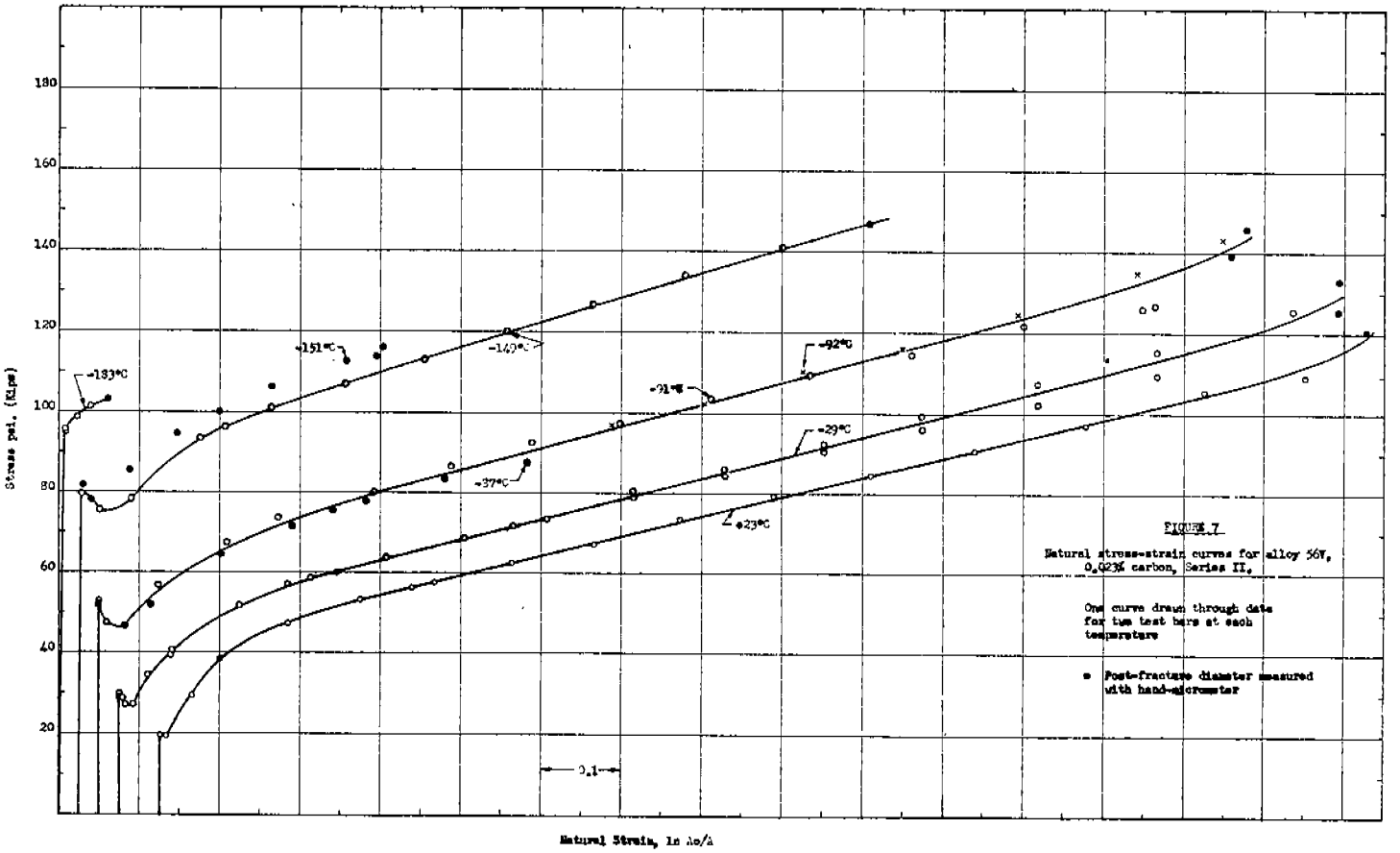

FIGURE 7
Natural stress-strain curves for alloy 56W, 0.02% carbon, Series II.

One curve drawn through data for two test bars at each temperature

• Post-fracture diameter measured with hand-micrometer

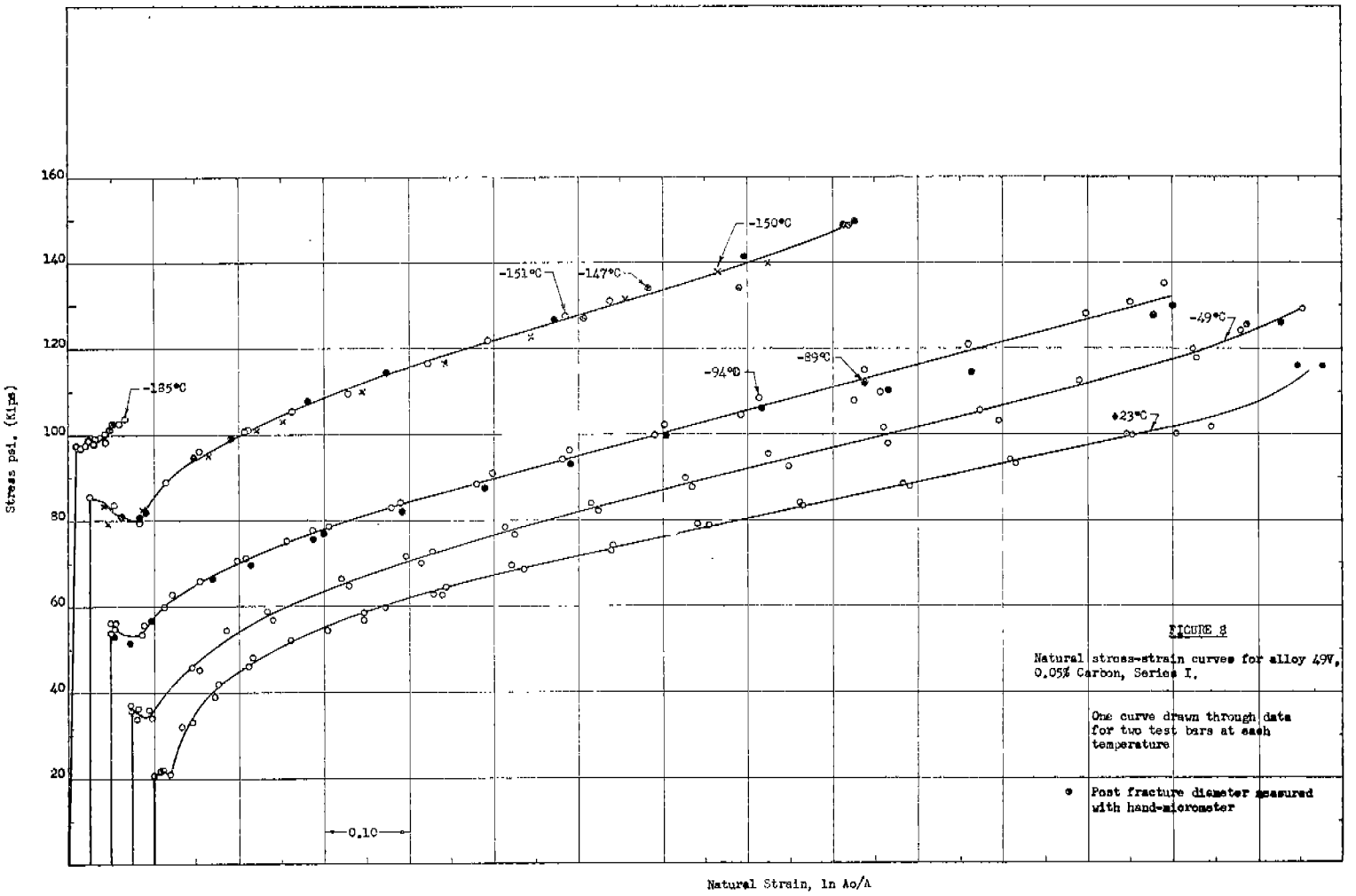

FIGURE 8

Natural stress-strain curves for alloy 49V, 0.05% Carbon, Series I.

One curve drawn through data for two test bars at each temperature

● Post fracture diameter measured with hand-micrometer

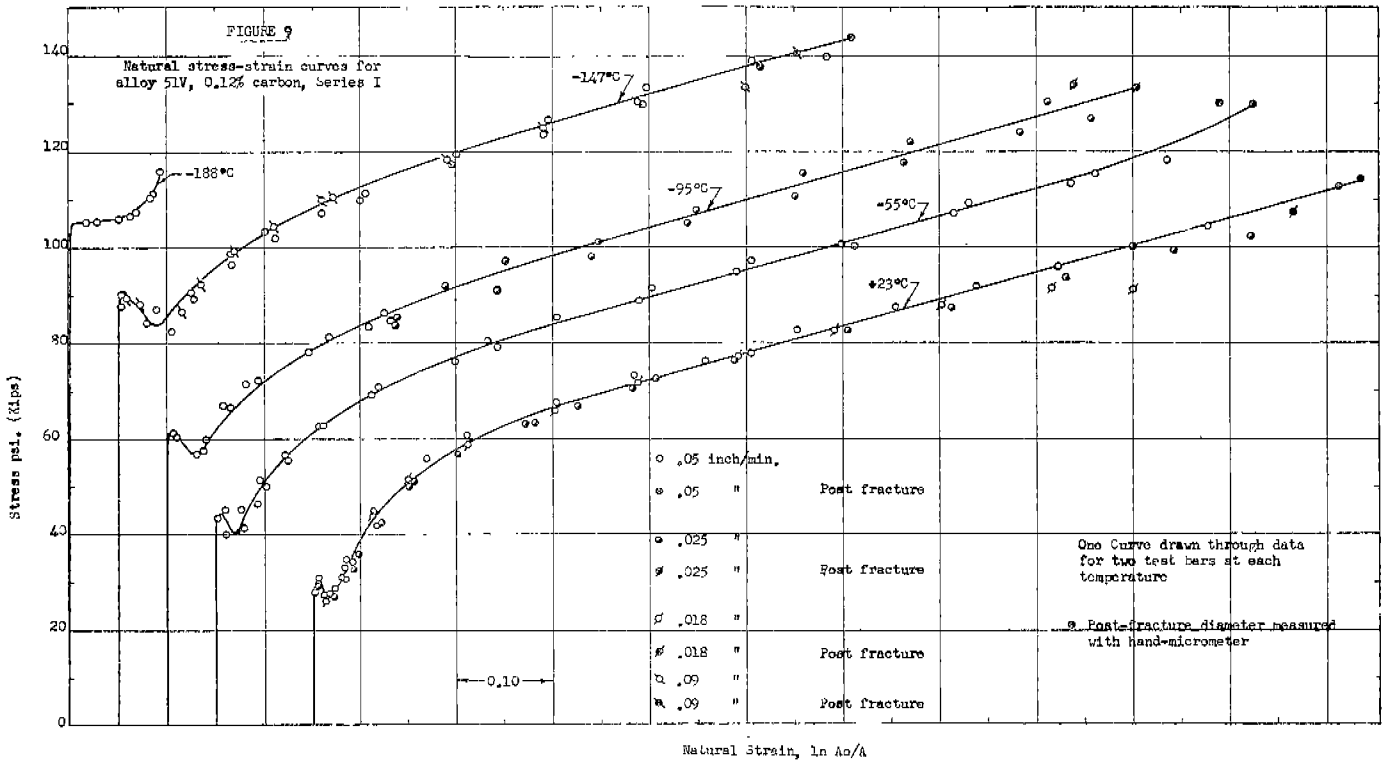

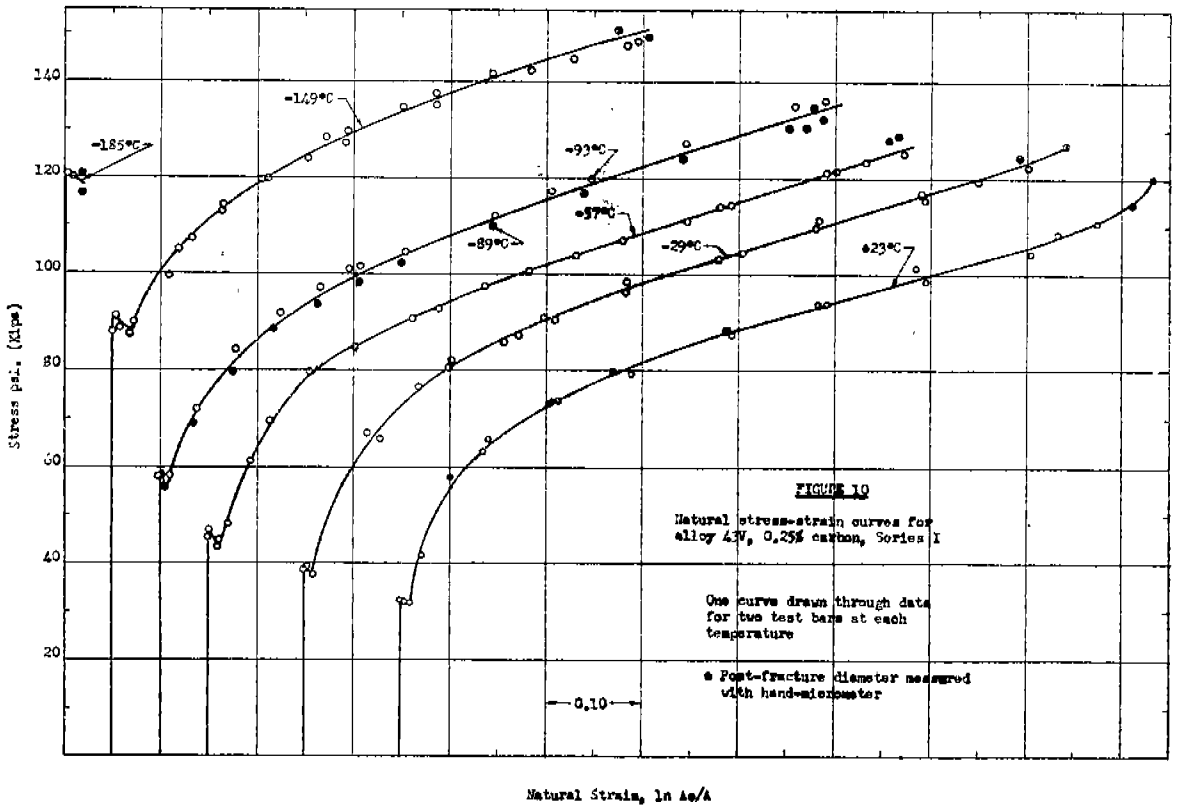

FIGURE 10

Natural stress-strain curves for alloy 43V, 0.25% carbon, Series I

One curve drawn through data for two test bars at each temperature

* Post-fracture diameter measured with hand-micrometer

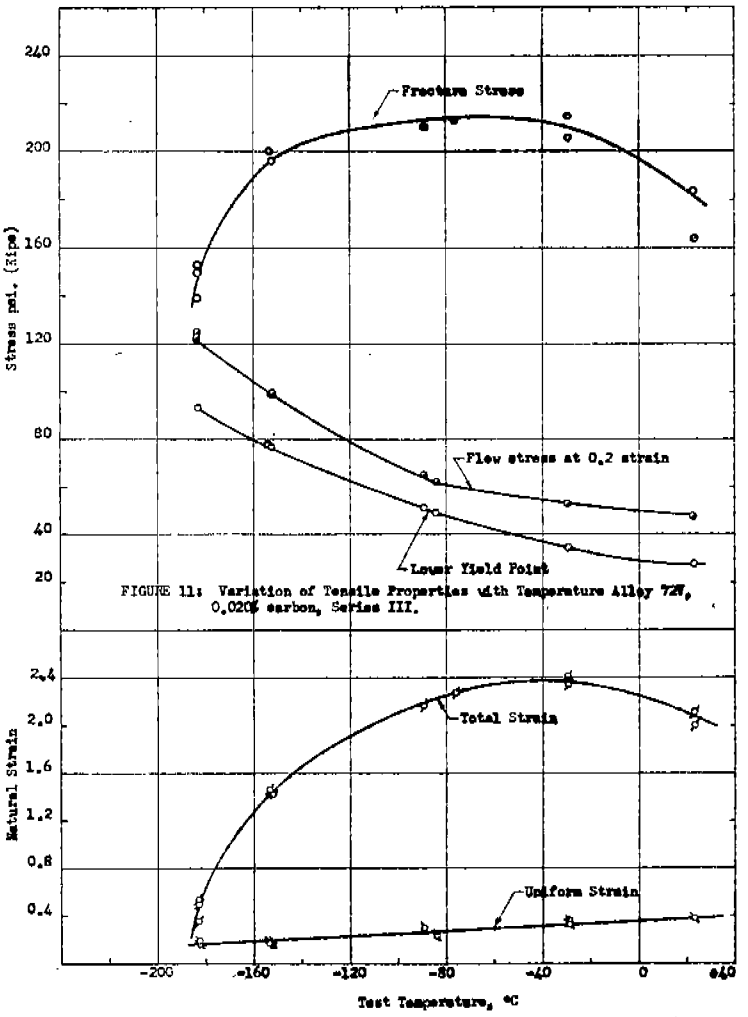

FIGURE 11: Variation of Tensile Properties with Temperature Alloy 72W, 0.020% carbon, Series III.

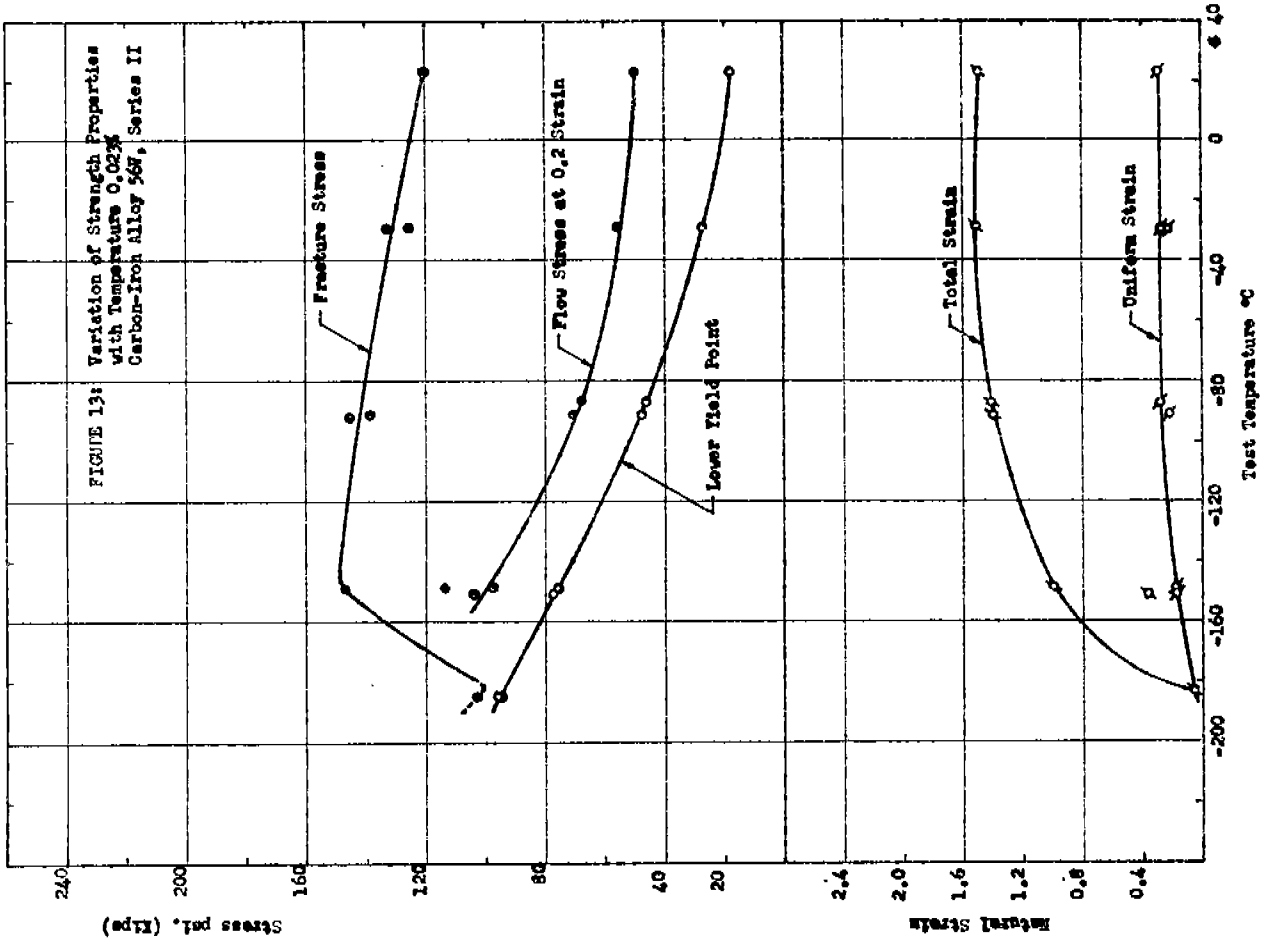

FIGURE 13: Variation of Strength Properties with Temperature 0,02% Carbon-Iron Alloy 56F, Series II

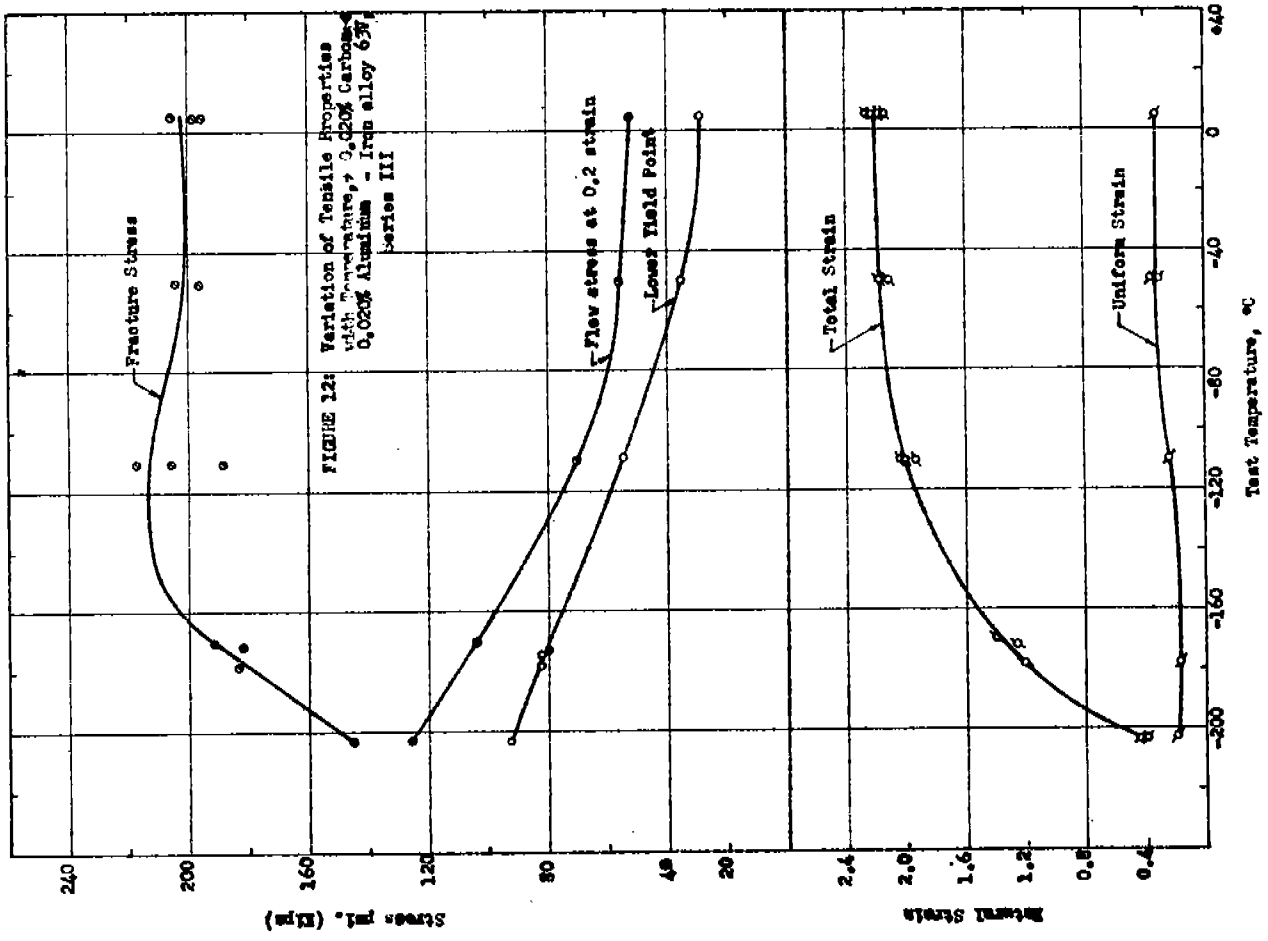

FIGURE 12: Variation of Tensile Properties with Temperature, 0,020% Carbon - 0,020% Aluminium - Iron alloy 67F, Series III

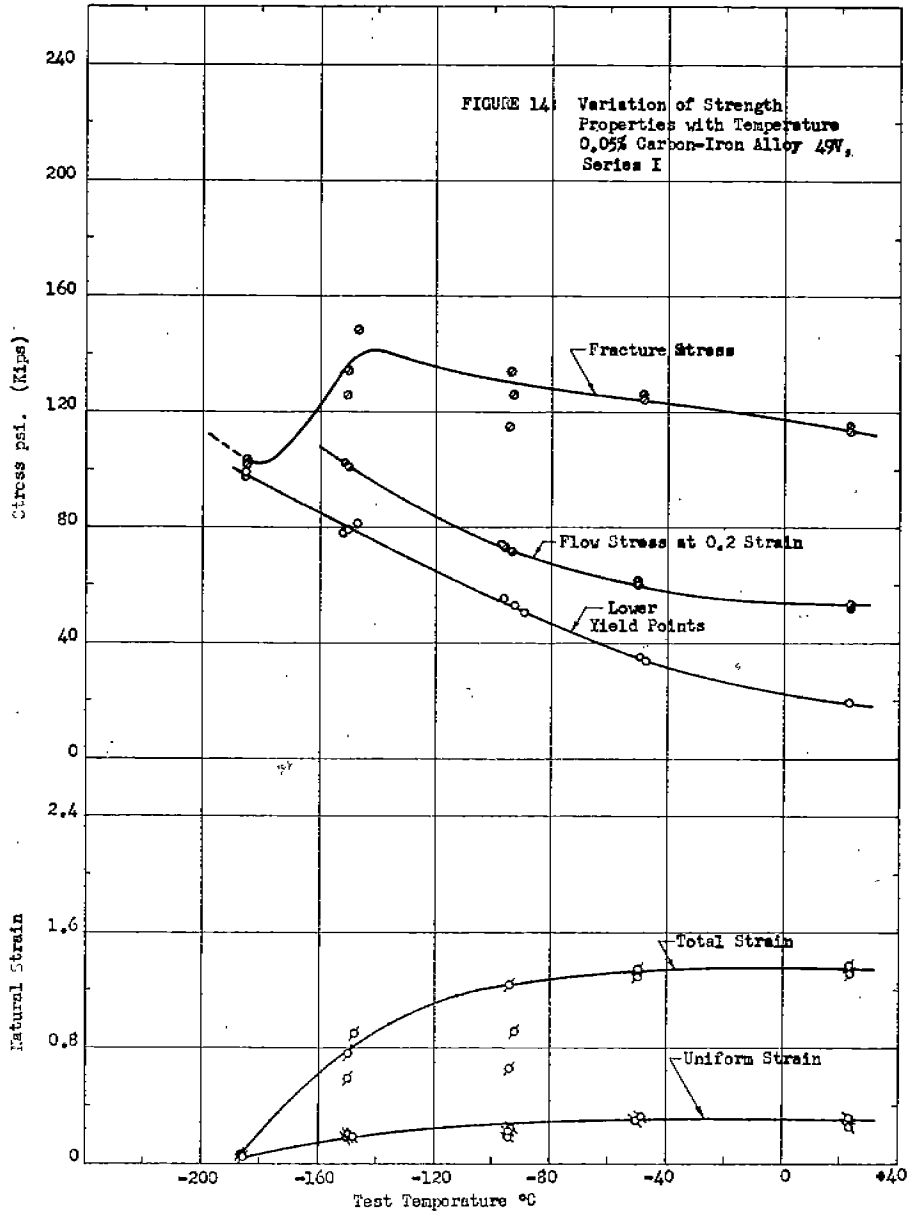

FIGURE 14: Variation of Strength Properties with Temperature 0.05% Carbon-Iron Alloy 49V, Series I

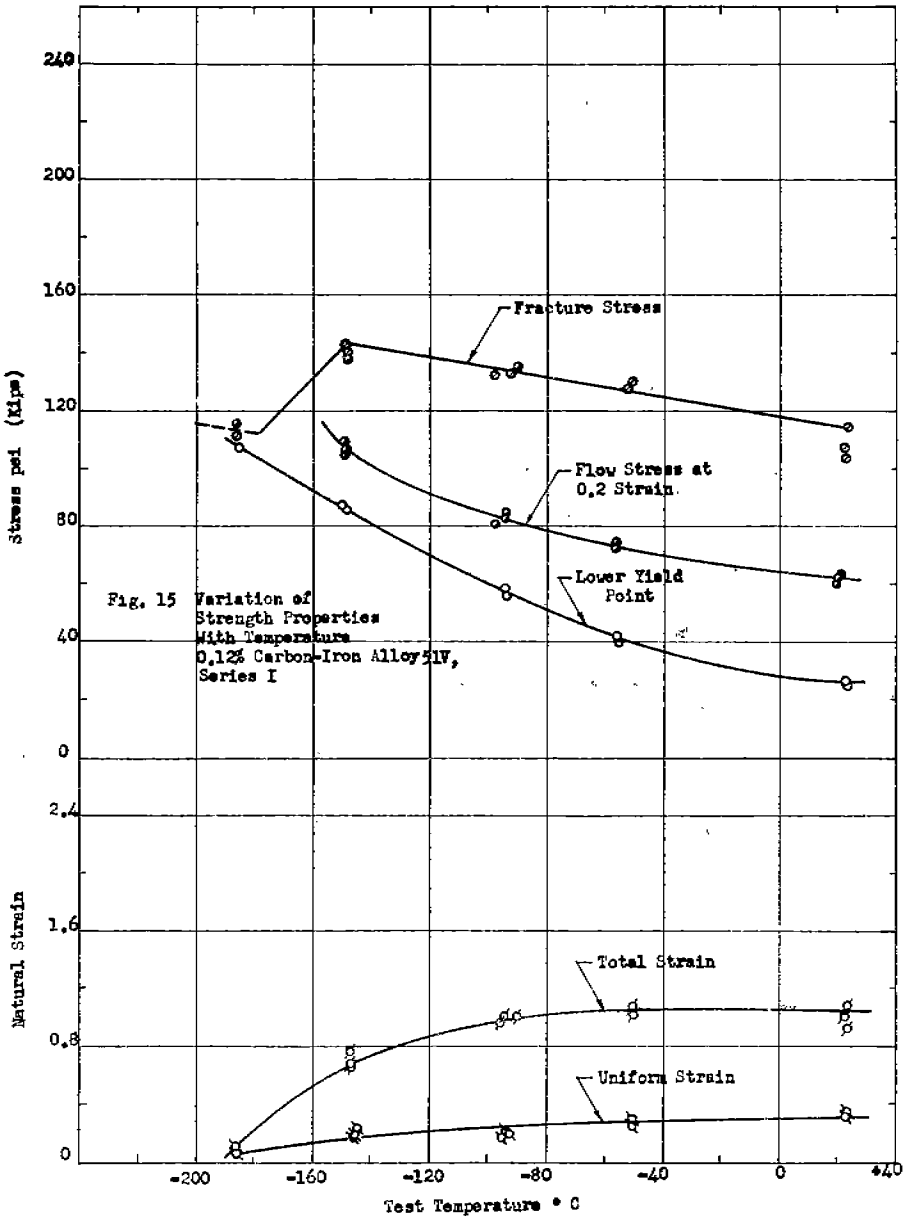

Fig. 15 Variation of Strength Properties With Temperature 0.12% Carbon-Iron Alloy 51V, Series I

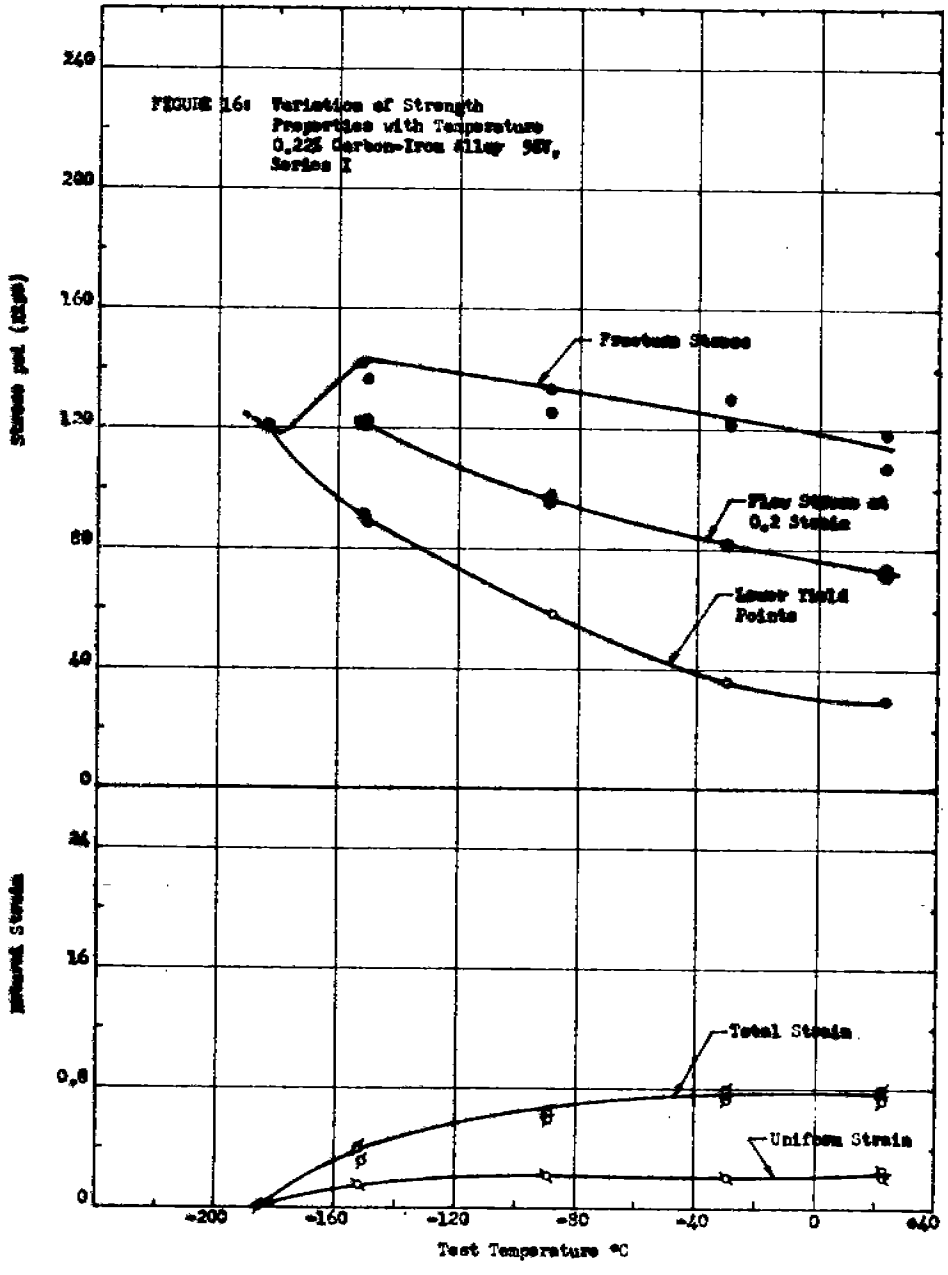

FIGURE 16: Variation of Strength Properties with Temperature 0,22% Carbon-Iron Alloy 56W, Series I

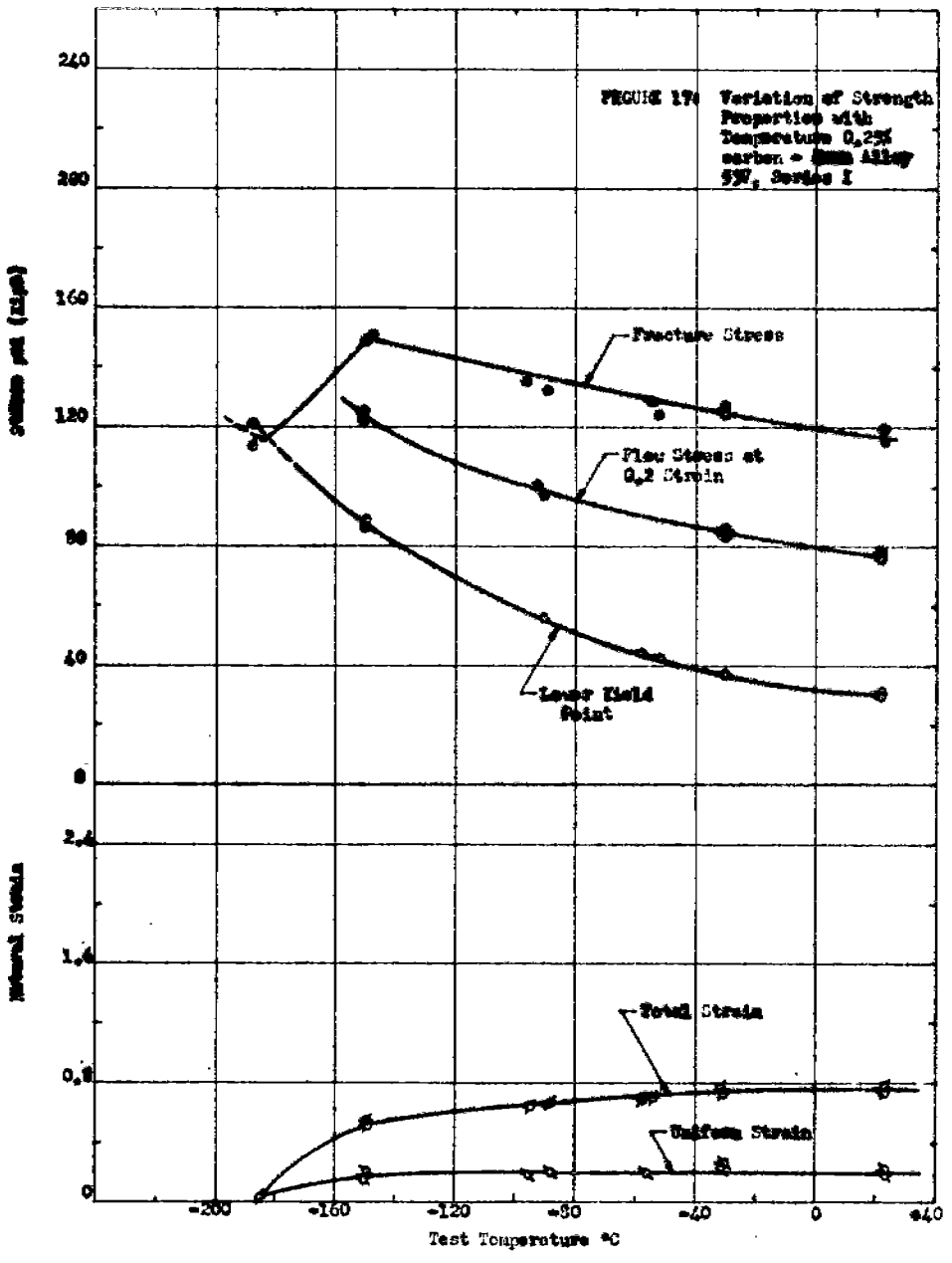

FIGURE 17: Variation of Strength Properties with Temperature 0,22% carbon - [illegible] Alloy 55W, Series I

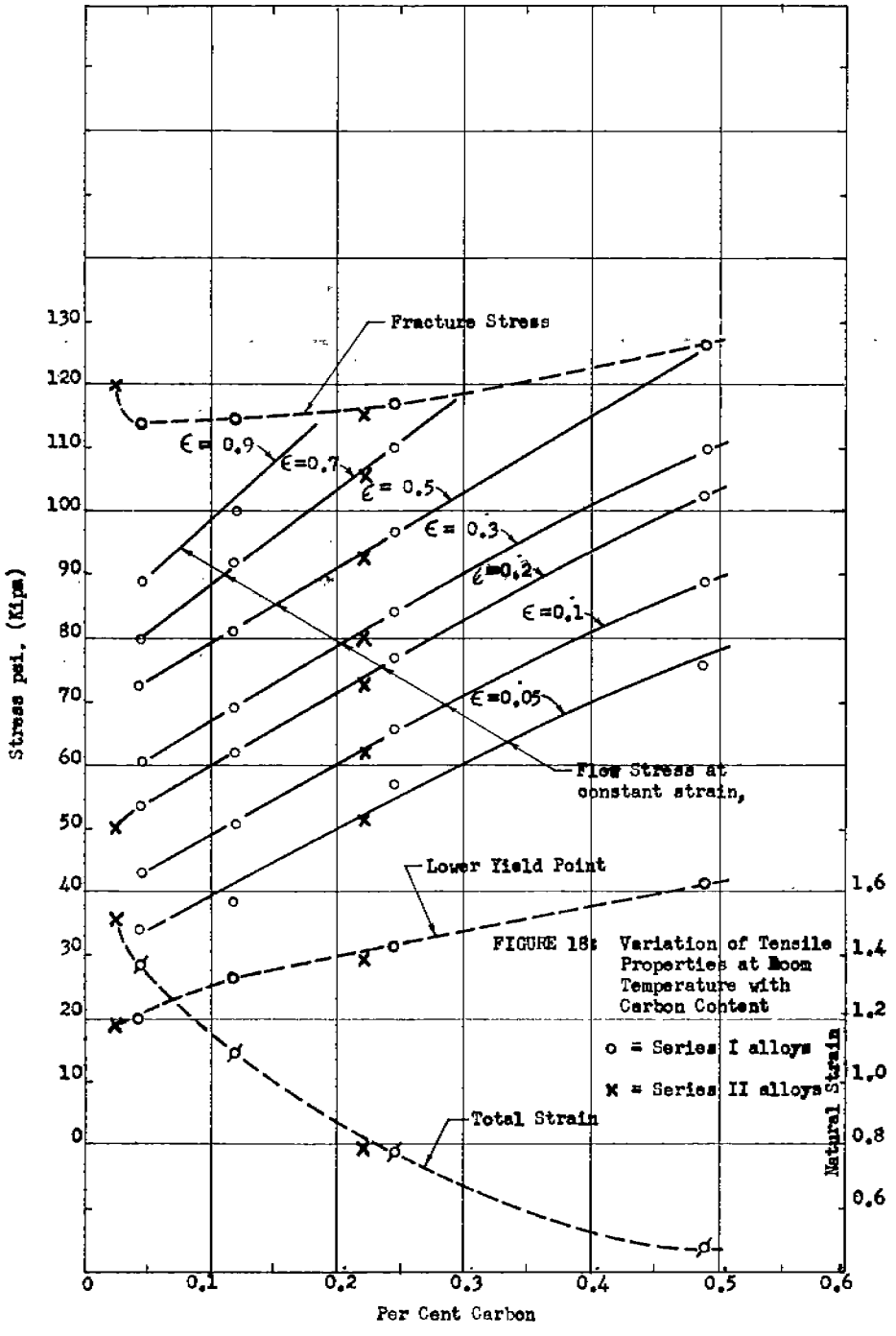

FIGURE 18: Variation of Tensile Properties at Room Temperature with Carbon Content

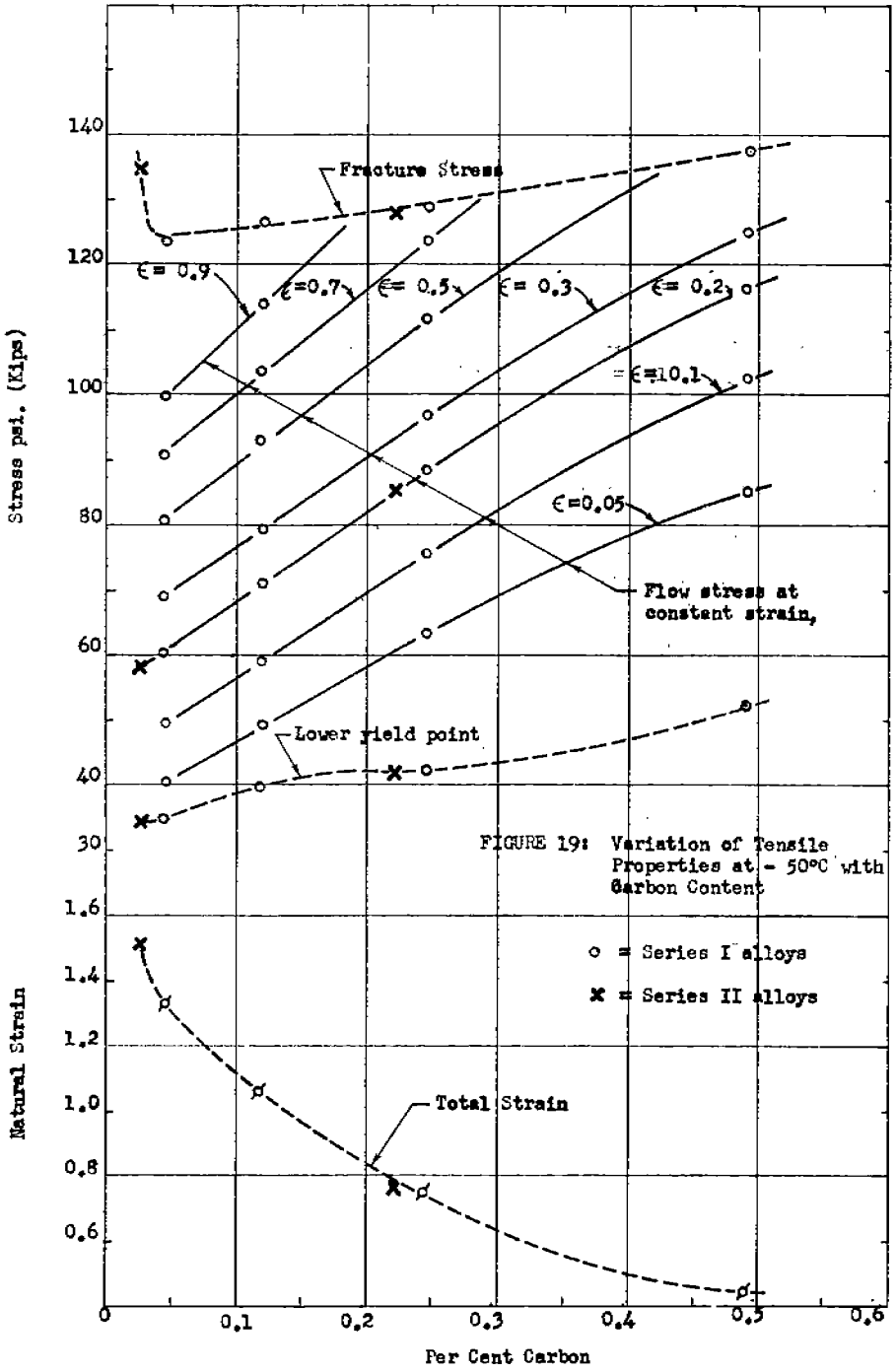

FIGURE 19: Variation of Tensile Properties at - 50°C with Carbon Content

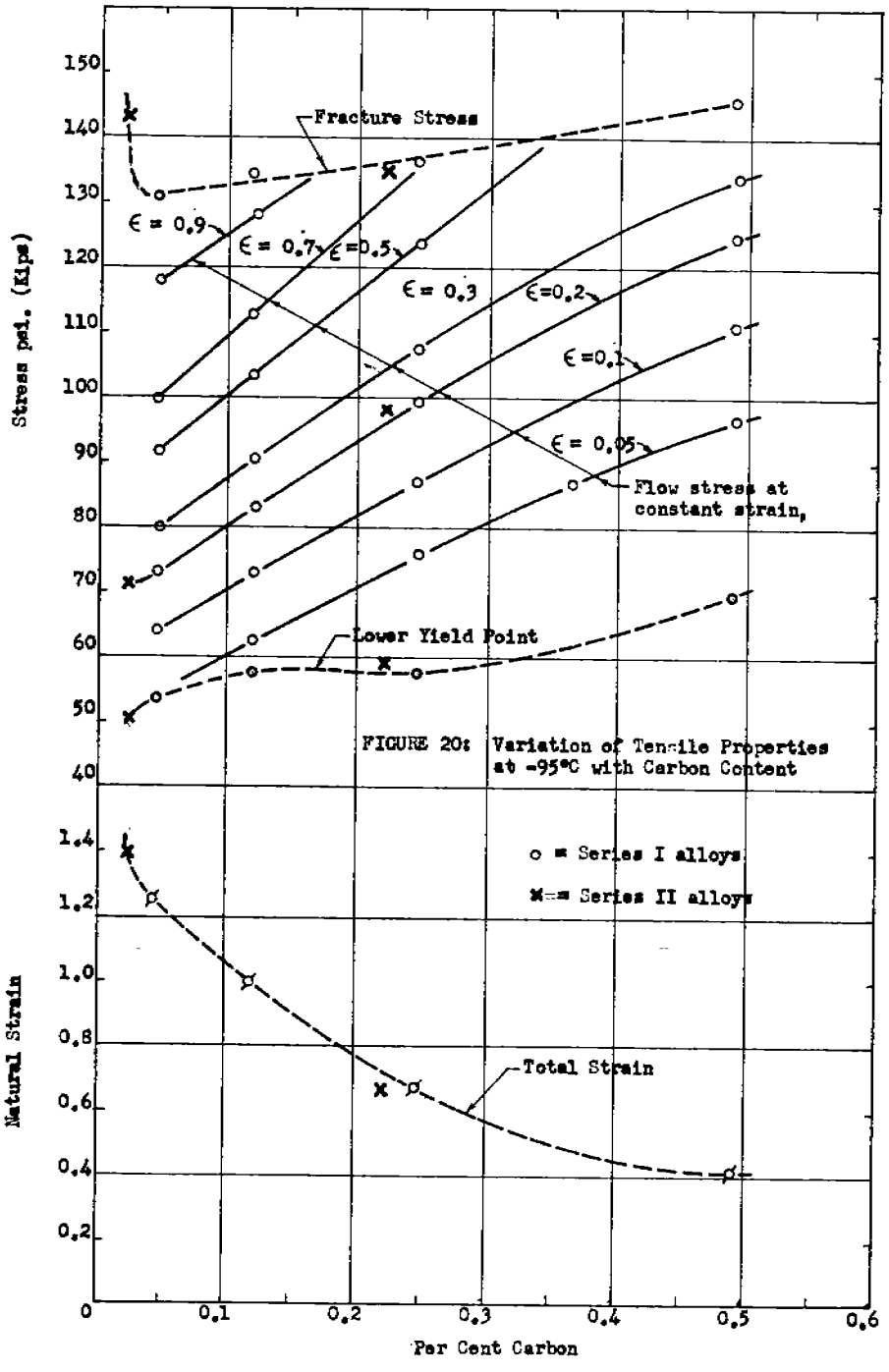

FIGURE 20: Variation of Tensile Properties at -95°C with Carbon Content

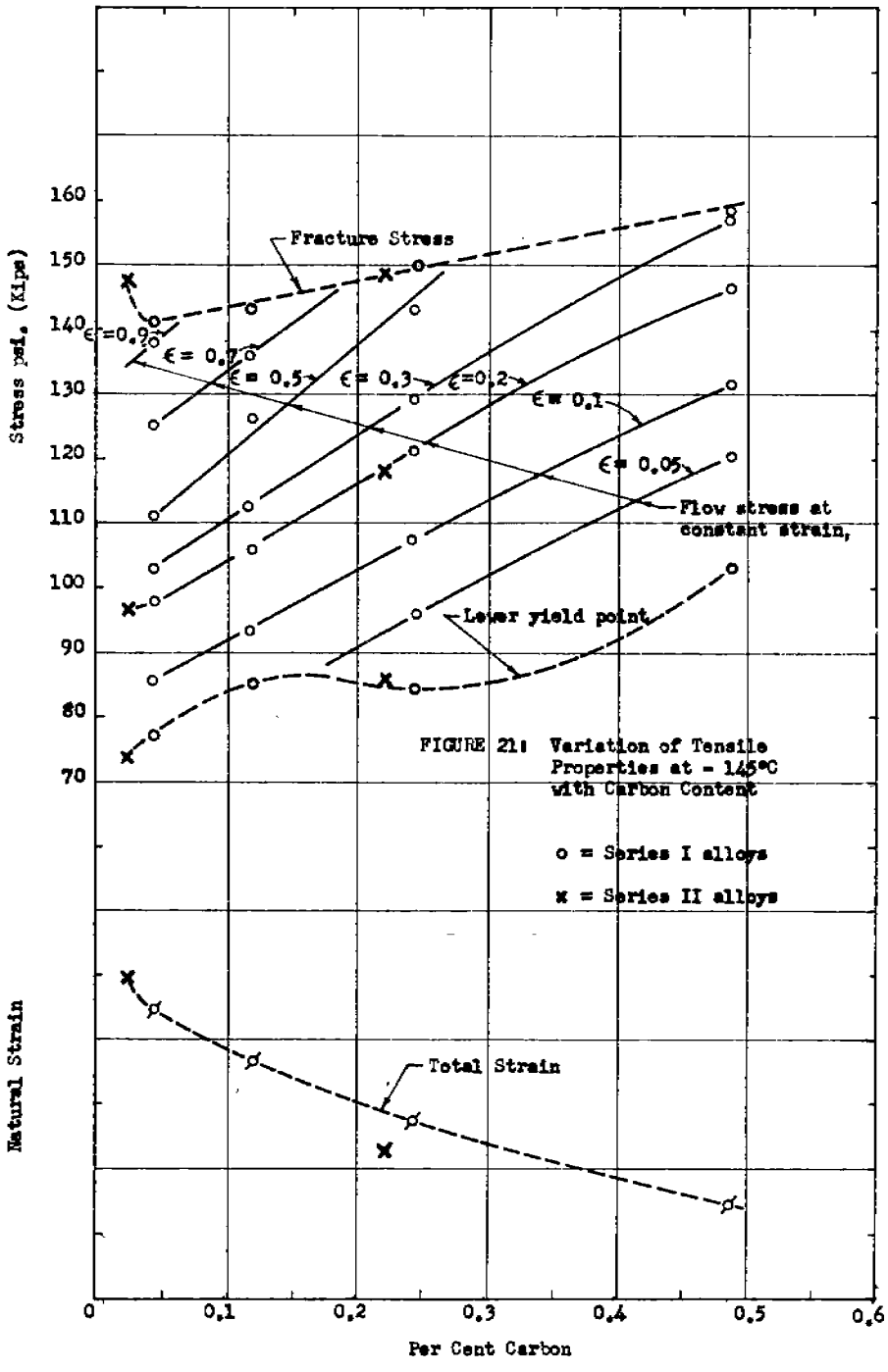

FIGURE 21: Variation of Tensile Properties at - 145°C with Carbon Content

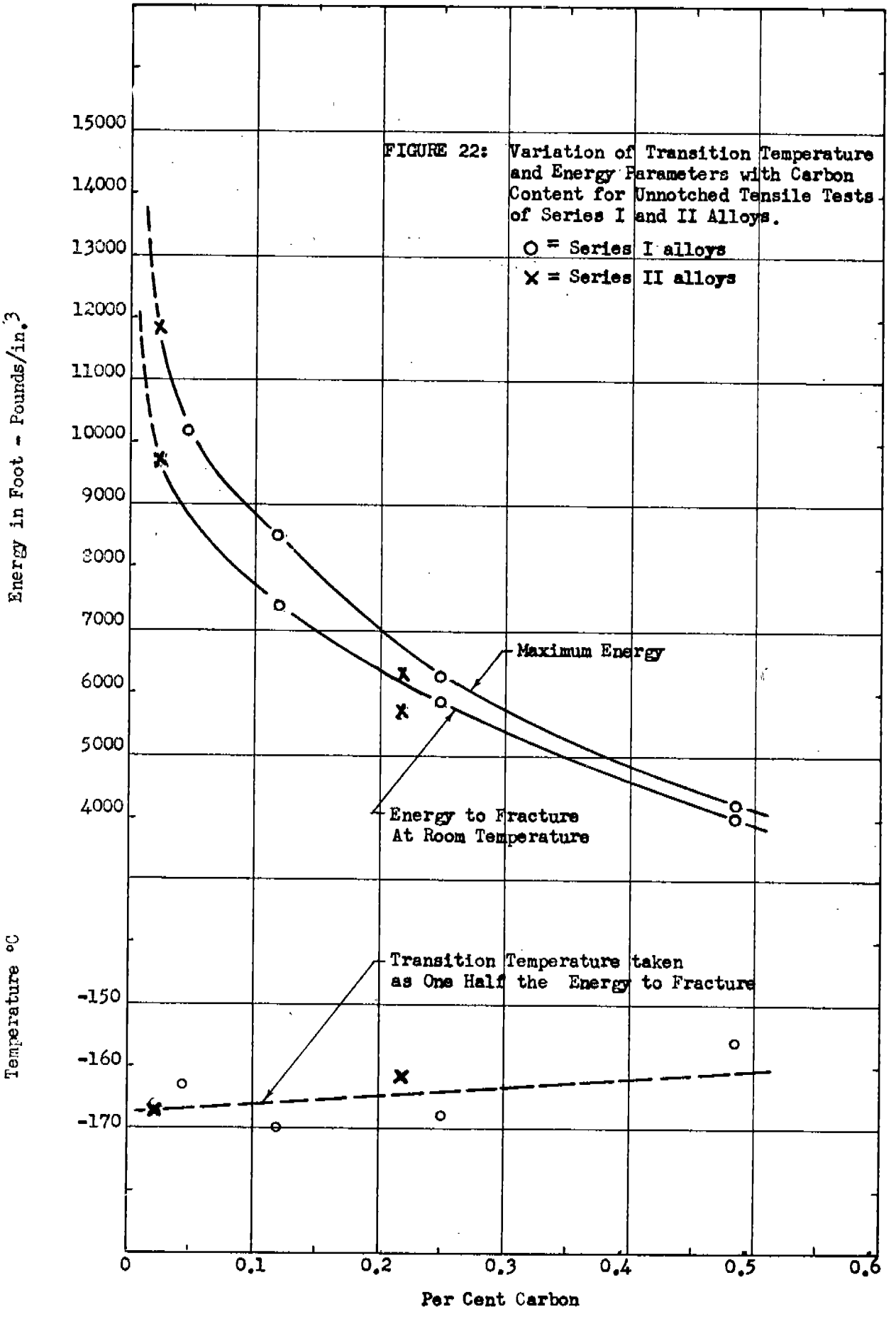

FIGURE 22: Variation of Transition Temperature and Energy Parameters with Carbon Content for Unnotched Tensile Tests of Series I and II Alloys.

O = Series I alloys

× = Series II alloys

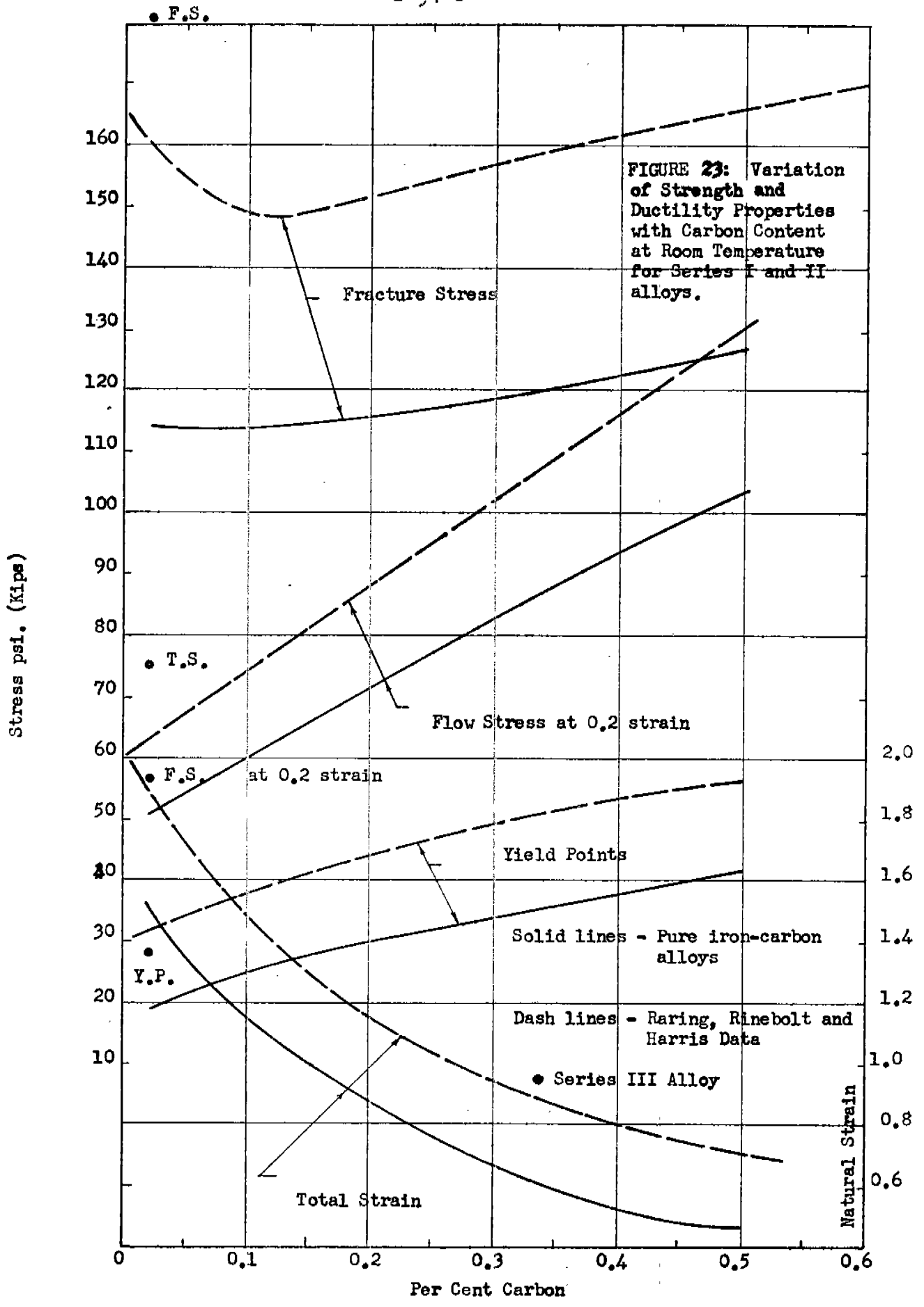

FIGURE 23: Variation of Strength and Ductility Properties with Carbon Content at Room Temperature for Series I and II alloys.

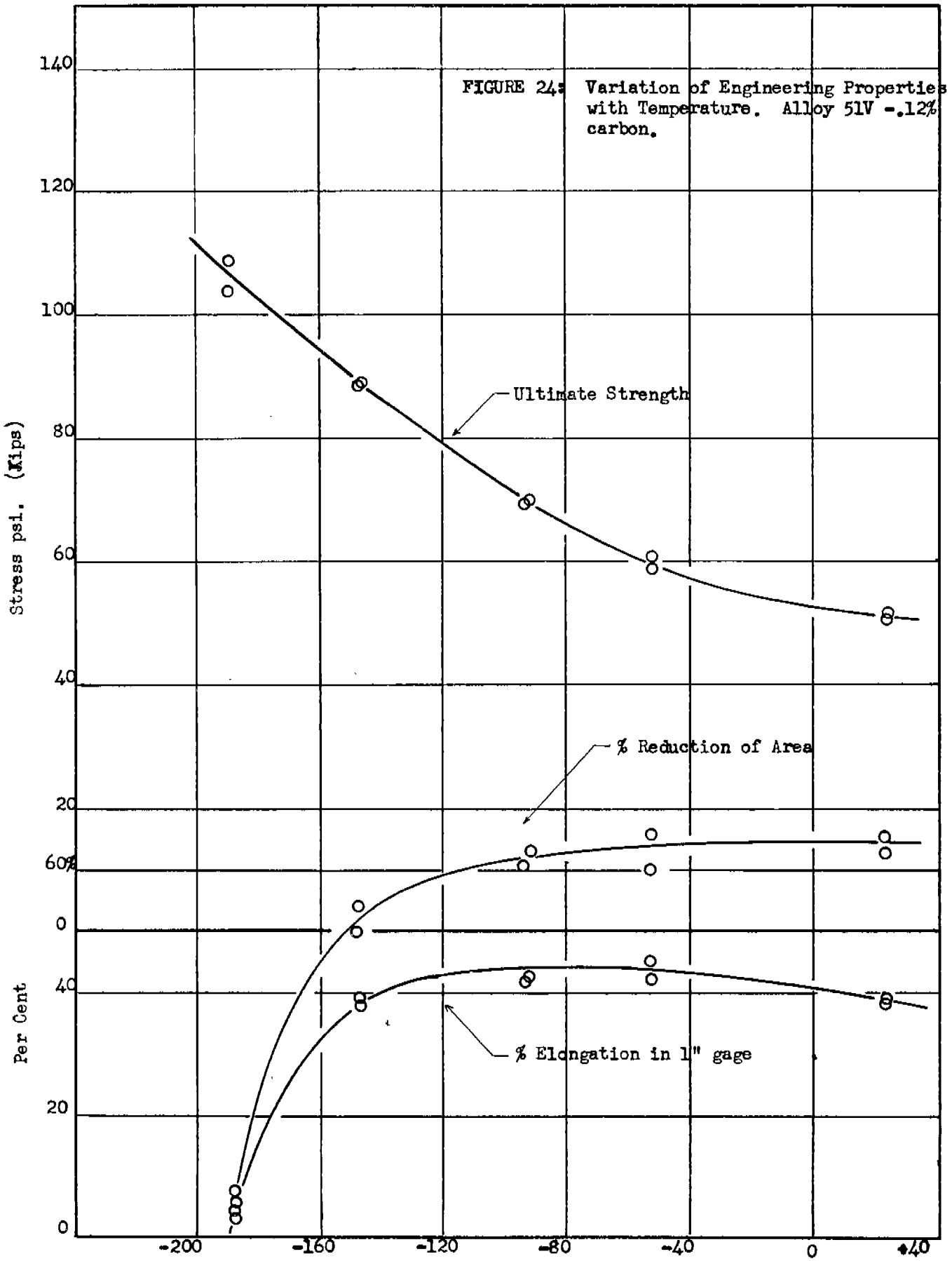

FIGURE 24: Variation of Engineering Properties with Temperature. Alloy 51V -.12% carbon.

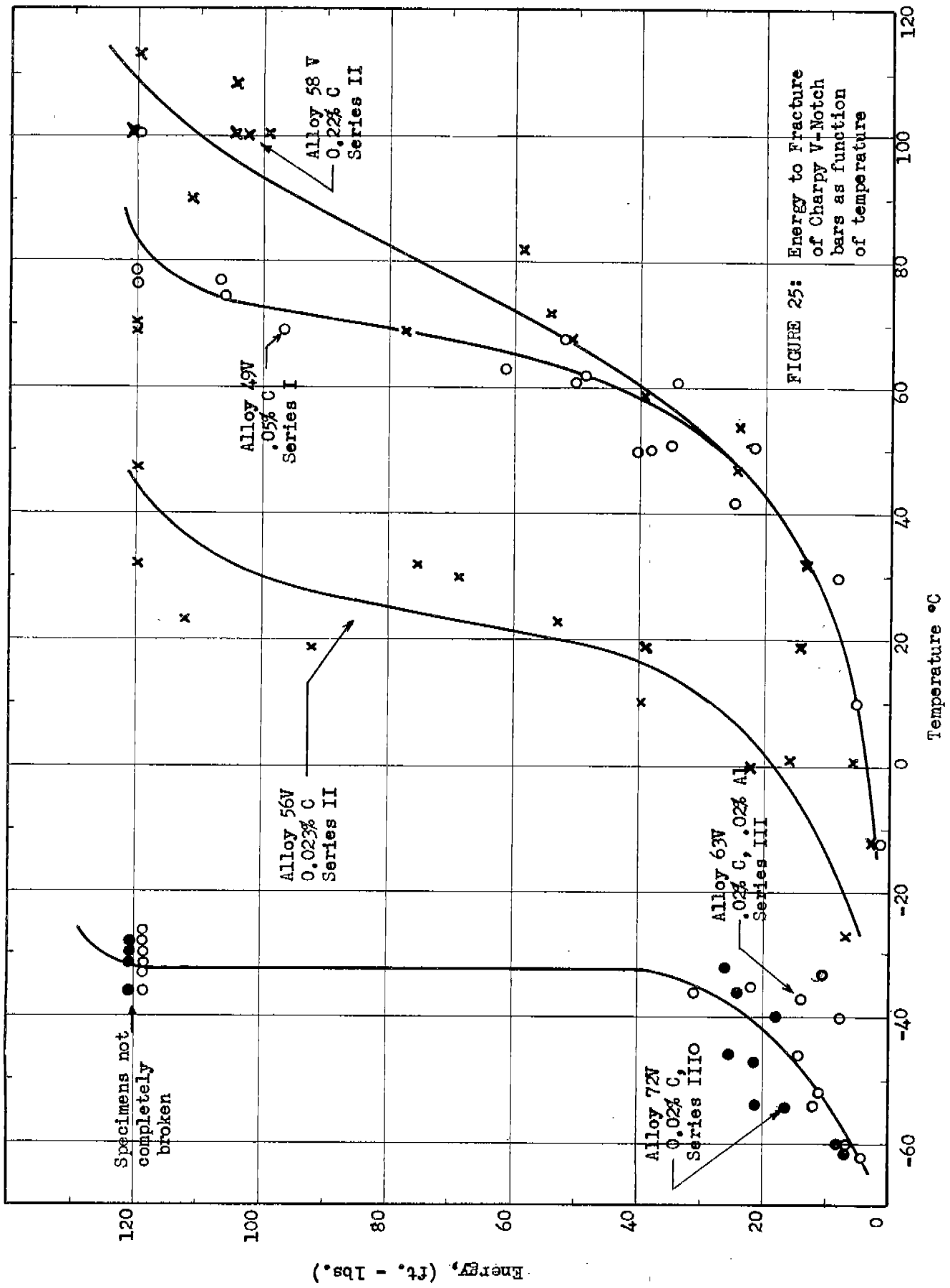
Energy, (ft. - lbs.)
Temperature °C
Alloy 58 W
0.22% C
Series II
Alloy 49W
.05% C
Series I
Alloy 56W
0.023% C
Series II
Alloy 63W
.02% C, .02% Al
Series III
Alloy 72W
0.02% C,
Series IIIO
Specimens not completely broken
Energy to Fracture of Charpy V-Notch bars as function of temperature

FIGURE 25: